The Journal of
Eukaryotic Microbiology

Published by the International Society of Protistologists

J. Eukaryot. Microbiol., 59(4), 2012 pp. 374–400

DOI: 10.1111/j.1550-7408.2012.00630.x

Studies on the Genus *Mesodinium* II. Ultrastructural and Molecular Investigations of Five Marine Species Help Clarifying the Taxonomy

LYDIA GARCIA-CUETOS,[a] ØJVIND MOESTRUP[a] and PER J. HANSEN[b]

[a]*Section of Marine Biology, Department of Biology, University of Copenhagen, Øster Farimagsgade 2D, DK-1353, Copenhagen, Denmark and*

[b]*Section of Marine Biology, Department of Biology, University of Copenhagen, Strandpromenaden 5, DK-3000, Helsingør, Denmark*

ABSTRACT. We provide a detailed study of four marine *Mesodinium* species and compare the data to the companion article on *Mesodinium chamaeleon* and other available studies on *Mesodinium*, to shed some light on the taxonomy of the genus. Micrographs of two red phototrophic *Mesodinium* species, *Mesodinium rubrum* and *Mesodinium major* n. sp., as well as the first published micrographs of two heterotrophic species, *M. pulex* and *M. pupula* are presented in combination with molecular analyses based on the ribosomal genes. The main conclusion of this study is the invalidity of the genus *Myrionecta* based on the arrangements of the basal bodies forming the cirri and the separation of species formerly known as *M. rubrum* resulting in an emended description of *M. rubrum* and the description of a related new species *M. major* n. sp.

Key Words. Ciliate, *Mesodinium, Myrionecta*, phylogeny, ultrastructure.

MESODINIUM species are found the world over in all types of aquatic habitats from freshwater to marine and from tropical to cold environments (e.g. Lindholm 1985) and exhibit a wide range of physiologies (i.e. strictly heterotrophic or mixotrophic, benthic or planktonic). Despite its exceptional plasticity, *Mesodinium* forms a well-defined genus light microscopically due to its conspicuous overall morphology. Species are composed of two hemispheres separated by a girdle where two ciliary belts are rooted. The oral ciliary belt is formed by polykinetids that extend into the water at 45, 90, and 135 degrees while the aboral belt is composed of rows of dikinetids that lie along the aboral part. Tentacles are present at the oral end (Lindholm 1985).

The best known species is *M. rubrum* (syn: *Myrionecta rubra*), which may form blooms responsible for spectacular red tides that are nontoxic and have been reported around the globe (Taylor et al. 1971). Yet, when comparing studies on strains and wild samples originating from distinct areas, different and sometimes even contradictory results emerge (Crawford 1993; Gustafson et al. 2000; Hansen and Fenchel 2006; Johnson and Stoecker 2005; Johnson et al. 2006, 2007; Park et al. 2007). The wide range of morphologies, physiologies, and ecological niches recorded in the literature about *M. rubrum* could indicate that several species are encompassed under the same species names. Herfort et al. (2011) investigated the genetic variability of *M. rubrum* in and near blooms in the Columbia River estuary and identified five different variants. However, only variant B was responsible for the blooms. Are the *M. rubrum* reported in the literature a species, a species complex or distinct species?

When going through the literature published on this particular species, there is a certain degree of confusion whether *M. rubrum* belongs to the genus *Mesodinium* Stein, 1863 or to the genus *Myrionecta* Jankowski, 2007. As a result, both generic names are currently in use (i.e. *Mesodinium rubrum* vs. *Myrionecta rubra*). This discrepancy has been at the heart of an ongoing debate since 1976 when the genus *Myrionecta* was first erected and *M. rubrum* was reassigned to the genus as *M. rubra*. Krainer and Foissner (1990) produced a key in which the photosynthetic *M. rubra* was separated from the nonphotosynthetic *Mesodinium* species. The key was based on generic descriptions and on previously published detailed ultrastructural studies of *M. rubrum* and light microscopical studies on *M. pulex* and *M. acarus*. However, Aescht (2001) pointed out that the name *Myrionecta* had not been described appropriately and was therefore invalid. Jankowski (2007) re-described the genus with *M. rubra* as its sole member, thus establishing a valid type species for the genus. He argued that *M. rubra* should be in a separate genus based on the arrangement of the kinetids. Yet no detailed ultrastructural studies of freshwater or heterotrophic species had been carried out at the time. Therefore, although many authors adopted the change, others kept referring to *M. rubrum*, pending additional information.

In an attempt to solve the generic position of *M. rubrum* and to look into its morphological and genetic variability, five marine species were studied in detail. They comprised three frequently found species in the waters of the Kattegat, Denmark (i.e. *M. chamaeleon, M. pupula*, and *M. major* n. sp.) and two species maintained in culture (i.e. *M. pulex* and *M. rubrum*). All species were investigated using light microscopy, scanning and transmission electron microscopy, and molecular techniques.

MATERIALS AND METHODS

Established cultures. A culture of the photosynthetic ciliate *M. rubrum* (Mr-DK2007) was established from single cells isolated from surface seawater samples collected at Frederikssund, Denmark, during a bloom event on 17 April 2007. The cryptophyte *Teleaulax amphioxeia* (K-0434, Scandinavian Culture Collection for Algae and Protozoa [i.e. SCCAP], Denmark) was used as prey.

A culture of the heterotrophic *M. pulex* was established from water samples collected from a boat launch near Shannon Point Marine Center, Washington, USA by Jakobsen et al. (2006). Growth in culture was maintained by feeding with the dinoflagellate *Heterocapsa rotundata* (K-0483, SCCAP, Denmark).

Crude cultures. Cells of *M. chamaeleon* were isolated from shallow waters at the sand surface in Nivå Bay, Denmark during the summers of 2007–2009 (Moestrup et al. 2012). When offered the cryptophyte *Chroomonas vectensis* as prey, the crude cultures could be maintained in the laboratory for several months.

Wild samples. *Mesodinium pupula* was found in a mix of sand and water collected in shallow waters in Nivå Bay during the summers of 2008–2009. The specimens were kept for weeks in the laboratory but then they died.

Mesodinium major n. sp. was found in water samples collected in the winter/early spring of 2008/2009 in the Sound between Helsingør and Copenhagen. Several attempts to

Corresponding Author: L. Garcia-Cuetos, Section of Marine Biology, Department of Biology, University of Copenhagen, Øster Farimagsgade 2D, DK-1353 Copenhagen, Denmark—Telephone number: +45 0 35 32 22 90; FAX number: +45 0 35 32 23 21; e-mail: garcia.lydia@gmail.com

establish it in culture by feeding it different cryptophyte species or small dinoflagellates failed.

Light microscopy. Live cells were observed using an Olympus IX-70 inverted microscope (Olympus, Tokyo, Japan) equipped with a differential interference contrast (DIC). Digital micrographs were taken with AxioCam (Zeiss, Oberkochen, Germany) or Canon EOS 40D (Tokyo, Japan) cameras when the cells were resting briefly. The motility patterns were recorded using an ordinary CCD camera (25 Hz frame rate) and with a high-speed CCD camera (CPL-MS100 CCD; Canadian Photonic Lab, Minnedota, Canada) with adjustable frame rates up to 1000 Hz.

Transmission electron microscopy. Fixations of the cells and preparation of the sections were carried out as described in Moestrup et al. (2012).

Scanning electron microscopy. Cell fixations were performed as described in Moestrup et al. (2012) on cultures of *M. rubrum* (Mr-DK2007) and *M. pulex*, mixed cultures of *M. chamaeleon*, and seawater samples containing *M. pupula* or *M. major* n. sp. All fixations were examined using a JEOL JSM-6335F field emission scanning electron microscope (JEOL, Tokyo, Japan) operated at 12 kV.

DNA extraction, single-cell isolation, PCR amplification, and sequencing. Prior to extraction, the cultures were starved for a week until all prey items had been depleted, and cells were checked under the light microscope for presence or absence of prey in the culture. Subsequently, the DNA extractions of cultures of *M. pulex, M. rubrum* (DK-2007), and *M. chamaeleon* were performed as previously described in Hansen et al. (2003).

Lugol-fixed cells of *M. major* and *M. pupula* were isolated using drawn Pasteur glass pipettes under an Olympus inverted microscope CKX31 (Olympus, Tokyo, Japan), and washed at least three times in ddH_2O under the inverted microscope to avoid any cryptophyte present in the fixed sample being carried over with the cell of interest. Finally, one washed *M. major* cell and five *M. pupula* cells were transferred into single 0.2 ml PCR tubes (StarLab, Ahrensburg, Germany) and kept frozen at −20 °C until further processing.

PCR amplifications were carried out in 50 μl. PCR amplifications of the small subunit ribosomal DNA, the ITS region, and part of the large subunit ribosomal DNA were carried out with the following primer combinations: 4617F and UNIDEUK670R (Johnson et al. 2004), 4617F (Bowers et al. 2006) and UNIDEUK1416R (Johnson et al. 2004), and finally UNIDEUK880F (Johnson et al. 2004) and D3B (Nunn et al. 1996). For single-cell isolations, a semi-nested PCR was carried out with the combination UNIDEUK880F and D2C (Scholin et al. 1994).

PCR amplification of the chloroplast fragment containing the partial 16S rDNA, tRNA-Ile gene, the tRNA-Ala gene, the Intergenic Transcribed Spacer (ITS), and the partial 23S rDNA and the nucleomorph LSU rDNA were carried out as described by Garcia-Cuetos et al. (2010). These amplifications were carried out to identify the origin of the plastids of *M. chamaeleon* and *M. major*.

All DNA fragments were purified using Nucleofast, following the manufacturer's recommendations (Macherey-Nagel Inc., Düren, Germany). Then, 500 ng of PCR product were air-dried over night and sent to the sequencing service at Macrogen (Seoul, Korea) for determination in both directions using the same primers used for amplification and assembled with Chromas pro (Technelysium Pty. Ltd., Brisbane, Australia).

Alignments and phylogenetic analyses. Three data sets of sequences were analysed. All sets were first aligned using MAFFT 6.624 (Katoh and Toh 2008) and then improved manually using BioEdit 7.0.5 sequence alignment software (Hall 1999). The first set was composed of 63 small subunit (SSU) rDNA sequences of freshwater and marine *Mesodinium* species. Five freshwater *Mesodinium* environmental sequences were chosen as outgroup based on Bass et al. (2009). Six of the marine species were obtained during this study while all others were retrieved from GenBank. A preliminary alignment and phylogenetic analyses were carried out to test alignments of different lengths and sample size. Environmental sequences that were too short or created noise were discarded. The second set comprised the six SSU rDNA, ITS region, and partial LSU rDNA (rDNA block) sequences of the marine species investigated in this article. To avoid the long branch attraction artifact and low bootstrap support, no outgroup was used due to the high divergence of *Mesodinium* sequences compared to other ciliates and alveolates available on GenBank (Johnson et al. 2004; Strüder-Kypke et al. 2006). Finally, the third alignment was built adding our sequences of *M. rubrum*, *M. major*, and *M. rubrum* from Antarctica to 158 environmental sequences published in Herfort et al. (2011). Our sequence of *M. chamaeleon* was used as outgroup. The sequences included the end of the SSU rDNA, the ITS region, and the beginning of the LSU rDNA (i.e. ITS block).

A Bayesian method was used to infer phylogeny, using the program MrBayes v.3.2 (Huelsenbeck and Ronquist 2001). Two simultaneous Monte Carlo Markov chains (MCMC) (Yang and Rannala 1997) were run from random trees for a total of 2,000,000 generations (i.e. metropolis-coupled MCMC). One of every 50 trees was sampled. Are we there yet (AWTY) software (Wilgenbusch et al. 2004) was used to graphically evaluate the extent of the MCMC analysis. After excluding the first sampled trees categorized as the "burn-in period", a consensus tree was constructed using PAUP* 4.0. b10 software (Swofford 2002) based on 39,840 trees. Then, jModeltest (Guindon and Gascuel 2003; Posada 2008) identified under the Akaike information criterion framework as the best model the GTR + G model for the rDNA block alignment, TIM2 + G model for the SSU rDNA alignment, and TVMef + G for the ITS block alignment. Using these settings, a tree was reconstructed with the online version of the PhyML software (Guindon and Gascuel 2003) available on the Montpellier bioinformatics platform at http://www.atgc-montpellier.fr/phyml. Branch support was obtained from Bayesian posterior probabilities and bootstrap (100 replicates) in maximum likelihood analyses (Felsenstein 1981). The reliability of internal branches was assessed using the bootstrap method with 100 replicates (Felsenstein 1985).

RESULTS

Light microscopy. General morphology of the five species was studied by light microscopy. Micrographs were taken when cells were resting momentarily (Fig. 1–15) and movies were made for studies of movement (Table 1). For all species, the position of the cirri and rows of dikinetids were identical in resting cells. In lateral view the cirri emerged at three different angles, forward, backward or perpendicular to the long axis of the cell. The dikinetids rested along the aboral half covering most of it. Division stages were similar in all five species. Division starts at the level of the two ciliary belts but we failed to determine whether the sister cells shared the belts of the mother cell or one cell inherited both belts and the other made them de novo. Both sister cells formed a constriction between the two sets of belts (Fig. 7) until breaking free from each other.

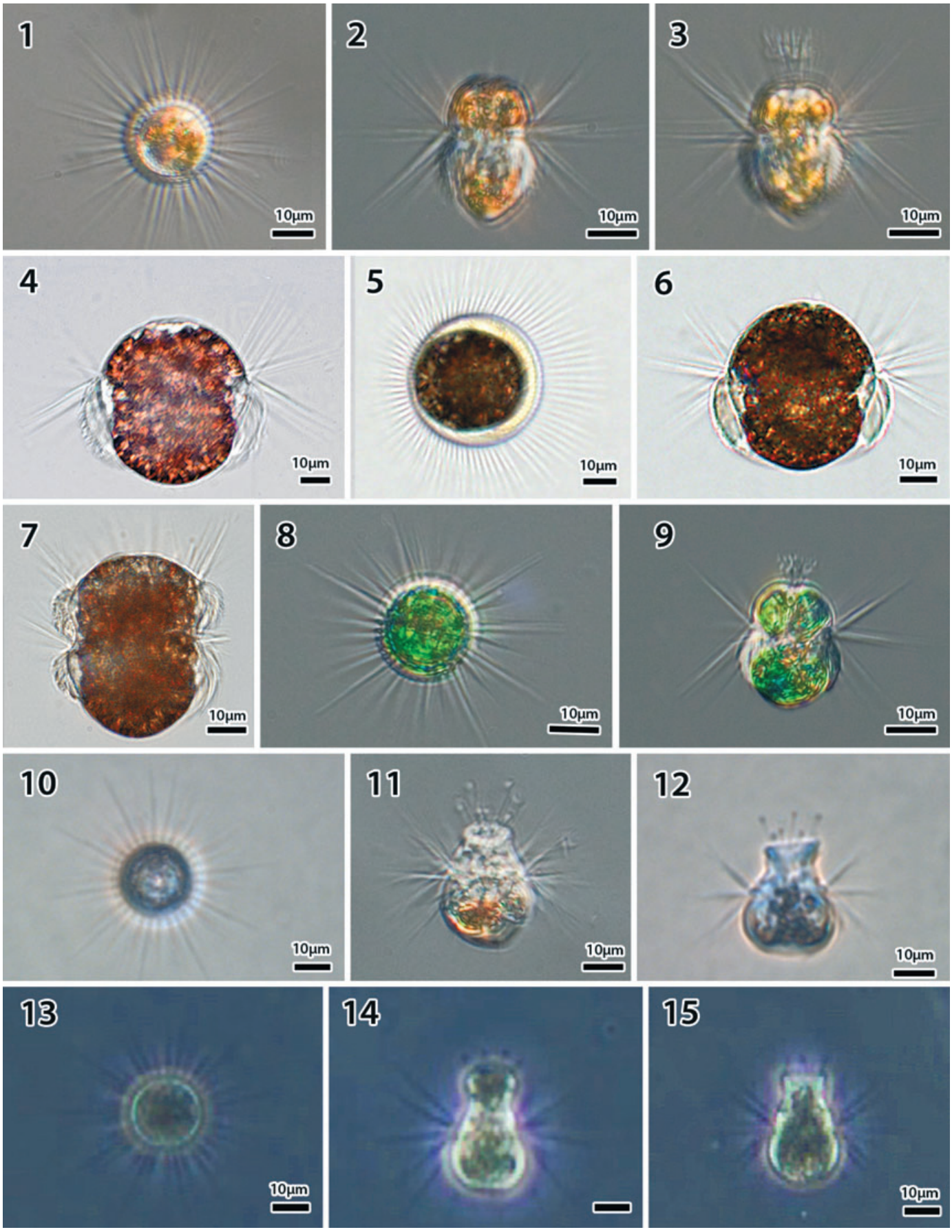
1
10μm
2
10μm
3
10μm
4
10μm
5
10μm
6
10μm
7
10μm
8
10μm
9
10μm
10
10μm
11
10μm
12
10μm
13
10μm
14
15
10μm

Fig. **1–15.** Light microscopy of *Mesodinium* species in apical and lateral view. **1–3.** *Mesodinium rubrum* cells of reddish-brown color with a rounded oral end and a conical aboral end. Cells are found without (2) and with tentacles (3). **4–7.** *Mesodinium major* n. sp., cells of reddish-brown color with a flattened oral end and a rounded aboral end. Typical division stage frequently found in growing populations (7). **8, 9.** *M. chamaeleon* cells displaying a bright green color and bearing tentacles. The oral end is slightly shorter than the aboral end. **10–12.** *Mesodinium pulex* with conspicuous cytostome and conical oral end, bearing 7–9 tentacles. Reddish food vacuoles are present in fed cells (11). **13–15.** *M. pupula* cells are pear-shaped. Three to five tentacles can be seen (14, 15).

Table **1.** Morphological and ecological characteristics of the live *Mesodinium* species in this study.

Species	Cell size	Chloroplasts	Symbiont nucleus	Motile behavior	Feeding strategy	Life style
M. pupula	L: 29 μm W: 20 μm	–	–	Swim, jump forward, crawl	Heterotrophic	Benthic
M. pulex	L: 27 μm W: 20 μm	–	–	Swim, jump forward, crawl	Heterotrophic	Planktonic/benthic
M. chamaeleon	L: 21 μm W: 13 μm	0–7	–	Swim, jump backward	Mixotrophic	Benthic
M. rubrum	L: 31 μm W: 21 μm	20	Present	Swim, jump backward	Phototrophic	Planktonic
M. major	L: 50 μm W: 40 μm	Many	Present	Swim, jump backward	Phototrophic	Planktonic

Mesodinium rubrum (Fig. 1–3 and Table 1) is 25–35 μm long and 16–25 μm wide ($n = 21$). The oral hemisphere is spherical while the aboral one has a conical shape. Six to eight tentacles are seen around the seemingly absent cytostome. It displays many chloroplasts that normally glow bright red in well-fed cells. The cells float in the water column and move by backward jumps.

Mesodinium major n. sp. (Fig. 4–7 and Table 1) is the largest species studied here, measuring 40–55 μm in length and 35–50 μm in width. Both ends are hemispherical but the oral is sometimes slightly flattened (Fig. 4, 6). The six to eight tentacles seen under the light microscope in the first few minutes of observation are quickly lost and therefore difficult to photograph. Cells harbor a large number of chloroplasts that are similar in color and shape to those of *M. rubrum*. The most striking ability of this species is to change the morphology of the oral hemisphere. When sampling specimens in winter, it sometimes flattened and produced flaps around the edge of the cell, the so-called "Medusa" form. Within the flaps, chloroplasts could be seen. After some time in the laboratory, cells reverted to the previously described morphology. *Mesodinium major* displays the same motility as *M. rubrum*.

Mesodinium chamaeleon (Fig. 8, 9 and Table 1) is 19–25 μm long and 13–17 μm wide ($n = 17$). Both hemispheres are rounded yet the oral end is shorter and narrower that the aboral end. The four to five tentacles usually seen display the typical distal and proximal mucocyst balls described in Moestrup et al. (2012) and rise clearly above the cytostome. In natural populations, green chloroplasts are present throughout the cell. The cells typically rest with the oral end downwards on the bottom, and may perform backward jumps in the water column.

Mesodinium pulex (Fig. 10–12 and Table 1) is 25–28 μm long and 16–25 μm wide ($n = 10$), with a typical conical oral end and a spherical aboral end, although variation occurred in the shape of the oral end due to stage of feeding (Fig. 11, 12). No chloroplasts were present yet colorful food vacuoles were observed. Usually six to eight tentacles were seen around the conspicuous cytostome (Fig. 11, 12). The cells spend most of the time vertically oriented and attached to the bottom (Fig. 10). Resting is interrupted by periodical motility. The cells swim forward, crawl on the substrate or perform small forward jumps.

Mesodinium pupula (Fig. 13–15 and Table 1) is slightly larger than *M. pulex* and displays a pear-shaped body with the hemispheres of even size. The cytostome is not as apparent as in *M. pulex* yet four to five short tentacles are often visible. The motile behavior is similar to *M. pulex* but the cells usually occurred near the bottom.

Ultrastructure. *Mesodinium rubrum* (Lohmann): The oral end was short and rounded and wider than the oval aboral end, and the ciliary belts appeared intercalated along the girdle (Fig. 18). A small cytostome was present, surrounded by tentacles that were divided into two parts (Fig. 19, 20). The proximal part of each tentacle was cylindrical while the distal part comprised four branches of extrusomes.

Cell division began by the cell growing in the longitudinal direction, and was followed by formation of an additional ring of polykinetids and dikinetids (Fig. 22). Endosymbionts were present throughout the cell and lacked the nucleus except immediately after having been ingested (Fig. 23, 24). Each dikinetid row was formed by up to 16 pairs of cilia (Fig. 23) but the number appeared somewhat variable (not shown). The kinetids have been illustrated at two different levels, showing 36 polykinetids (Fig. 24) and 40 dikinetids and cirri (Fig. 25).

The oral end was examined in detail, since this part of the cell was found to vary among species of *Mesodinium*. A total of 16 tentacles emerged from the cell (Fig. 26), each supported internally by an axoneme of 14 microtubules (Fig. 29). Within the cell each axoneme was accompanied by an additional axoneme, making a total of 32 axonemes (Fig. 27). The oral edge of the cell was supported by numerous rows of microtubules inserting between the tentacle axoneme pairs (Fig. 30). Centrally, the oral end contained a cytostome (Fig. 30). The proximal part of the tentacle contained only the axoneme ring of microtubules and was ~ 8 μm long (Fig. 28). Distally, the diameter of the tentacle increased (Fig. 34) and four extrusomes were inserted (Fig. 31–33). The axoneme terminated soon after the extrusomes diverged; each extrusome was usually surrounded by a membrane although the membrane was sometimes indistinct. Close inspection of the pairs of tentacle axonemes within the cell revealed that the second member of each pair lacked an emergent part and contained 11 rather than 14 microtubules (Fig. 35).

Near the cirri, each dikinetid row terminated with four naked (i.e. cilia-lacking) basal bodies or centrioles (Fig. 36–39). Two centrioles were located close to the oral-most dikinetid, herein designated the right pair of centrioles. The centrioles inserted at acute angles to each other (Fig. 38). Within each pair the angle was slight and could not be assessed (Fig. 36), but between pairs the angle amounted to ~ 60° (Fig. 38).

Each polykinetid comprised 16 basal bodies, arranged in four rows of 5, 5, 4, and 2 basal bodies arranged perpendicularly to the cell surface (Fig. 40, 41, see also the low

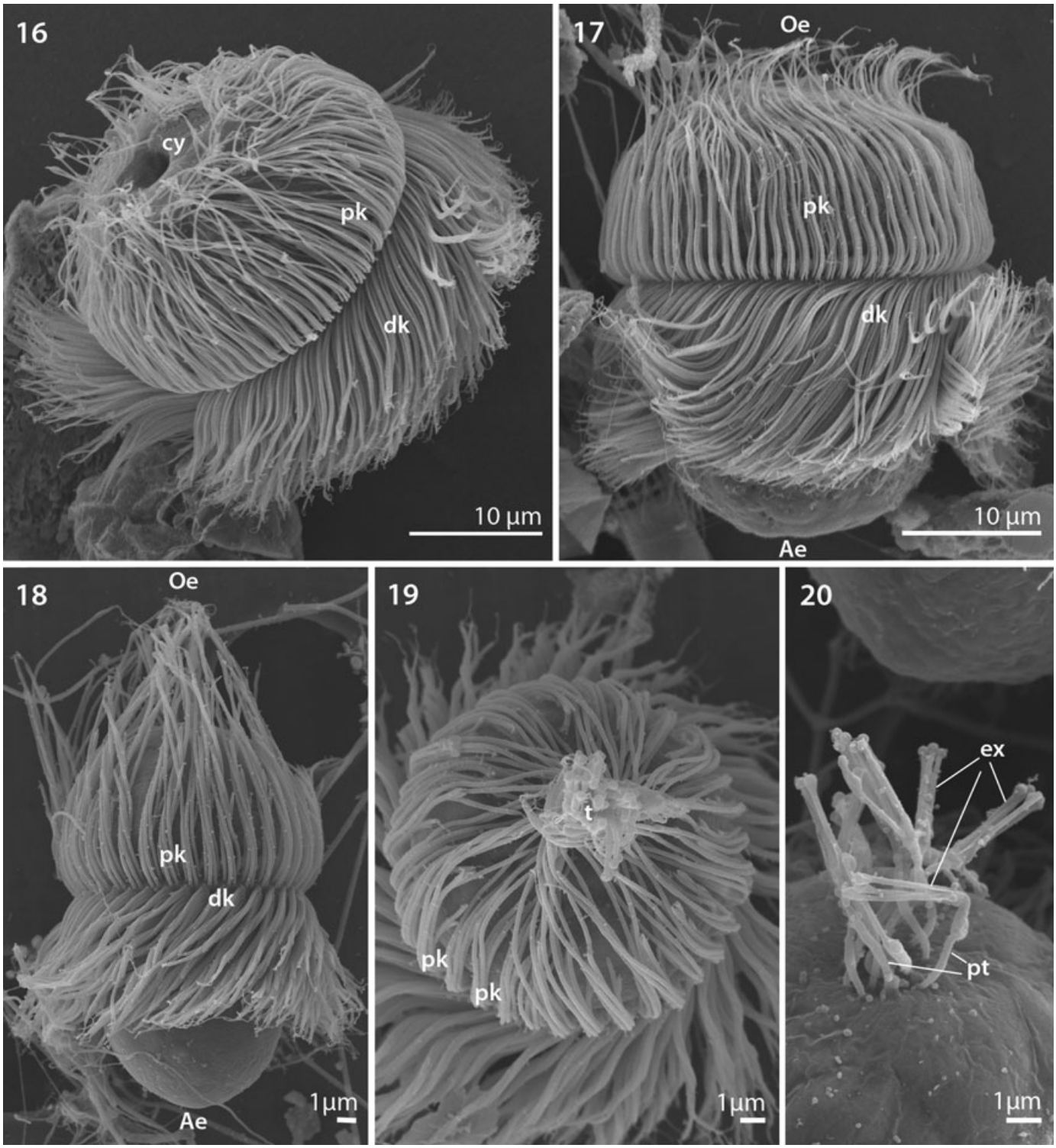

Fig. **16–20.** Scanning electron micrographs of *Mesodinium major* n. sp. and *Mesodinium rubrum*. **16–17.** *M. major* n. sp., cells displaying a great number of cirri (pk) and dikinetid rows (dk). The cytostome (cy) is conspicuous but no tentacles are present around it (16). **18–20.** *M. rubrum* cells in lateral view (18) and apical view. Tentacles can be seen but no cytostome (19–20). Tentacles consist of a proximal part (pt) bearing 2–4 extrusomes (ex) (20). Oe: oral end, Ae, aboral end

magnification Fig. 25). Eight of the 16 basal bodies extended into very short cilia (Fig. 42) whereas the other eight grew longer cilia, which merged to form a cirrus (Fig. 42, and at low magnification in Fig. 24). The eight cilia of a cirrus were arranged in a 7 + 1 configuration (i.e. seven surrounding a central cilium; Fig. 41, 42). This is particularly clear in Fig. 42

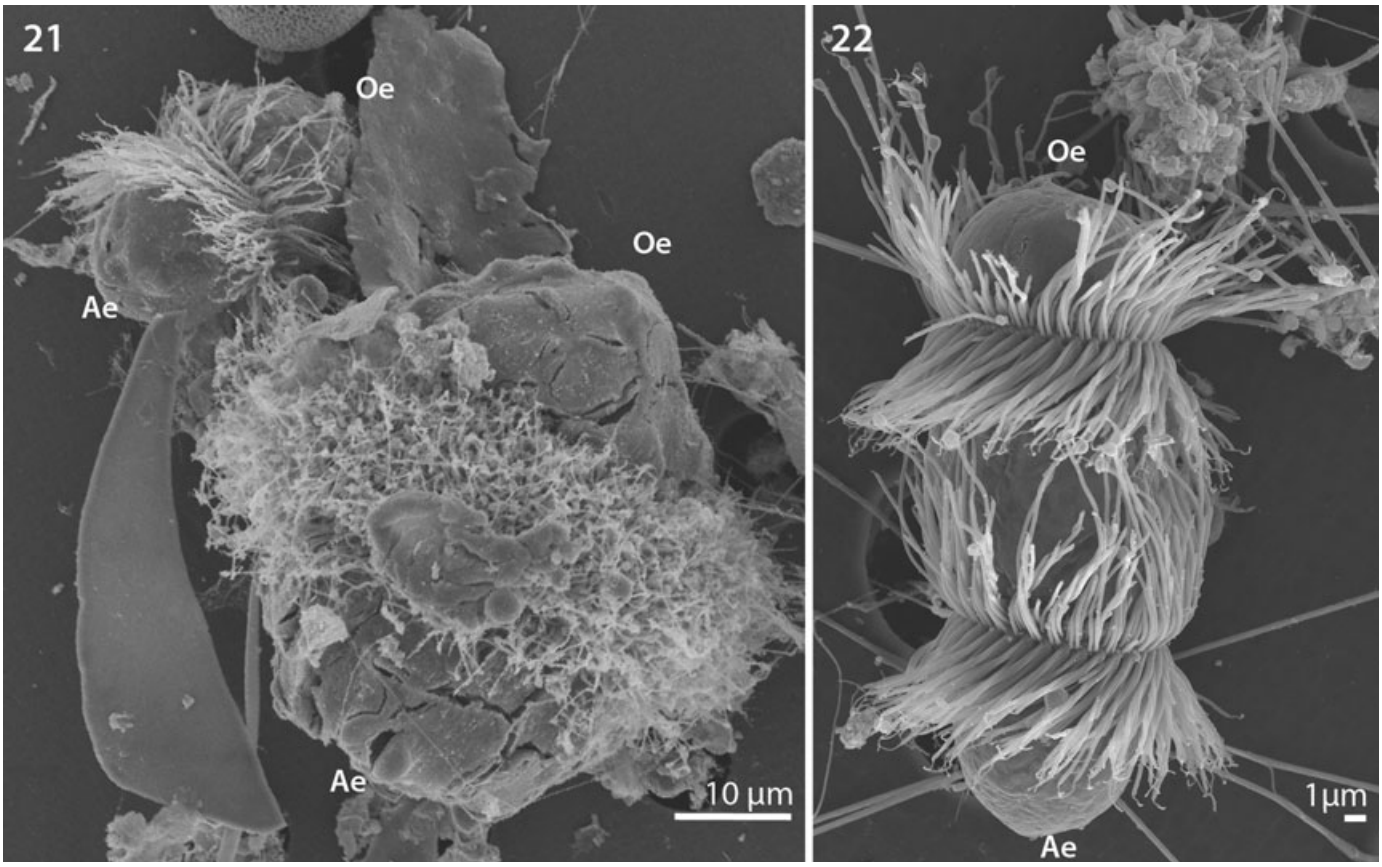

Fig. **21–22.** Scanning electron micrographs of *Mesodinium major* n. sp. and *Mesodinium rubrum*. **21.** Both species side by side in a water sample, *M. rubrum* is in the top left side. **22.** Cell of *M. rubrum* undergoing division in which replication of both sets of ciliary belts and elongation of the cell can be seen. Oe: oral end, Ae, aboral end

where the cirri that normally cover the eight short cilia at the base were shed by the cell before or during fixation, leaving only the bases of the cilia behind. The central one differed by being slightly swollen (arrowhead, Fig. 40, 41). Each cirrus was formed of cilia from three rows, as illustrated diagrammatically in Fig. 43.

Mesodinium major n. sp. Cells of *M. major* are characterized by their large size, large number of kinetids, and large cytostome (Fig. 16, 17, 21). Fixation and embedding were attempted on several occasions but the fixation quality, although sufficient to retrieve the data, did not provide satisfactory micrographs. *M. major* was identical to *M. rubrum* in structure of the polykinetids, dikinetids, supernumerary naked basal bodies (centrioles), and tentacles and also in the presence of endosymbionts, ciliate nuclei (two macronuclei and one micronucleus), and the presence of an endosymbiont nucleus. Differences include a very large cytostome in *M. major* (Fig. 16) and a much higher number of kinetids, assessed to be 70–80, and a higher number of endosymbionts (~ 40 – 60) (data not shown). In a cell serially sectioned transversely, the number of kinetids could be counted precisely as 75 (data not shown).

Mesodinium pupula Dragesco. Cells of *M. pupula* lack endosymbionts but food vacuoles are often visible (Fig. 44). The cells also contain large numbers of lipid droplets, and more or less spherical or ovoid vacuoles with grayish contents (Fig. 44, 45). The latter are surrounded by single membranes and appear to fuse with the cell membrane, thus releasing their contents to the exterior. The nature of this material has not been ascertained. We have not observed extended tentacles in the SEM and TEM. However, they were visible when filmed under the light microscope (not shown). In the material prepared for SEM and TEM, the oral end showed a ring of swellings (Fig. 44, 46, 47), which appears to represent tentacles that may have retracted as a result of fixation. Sixteen such retracted tentacles are visible in the cell sectioned transversely (Fig. 47). Distally, each tentacle swelling comprised two parts, while proximally they formed a single entity (Fig. 48, 50). Both parts contained four extrusomes, in addition to the axoneme (Fig. 47, 48, 50), and all axonemes contained 23 microtubules (Fig. 49). The outer part of the tentacle swelling also contained a band of microtubules (Fig. 48, 50), which apparently did not extend into the cell body (Fig. 50). The tentacle axonemes extended for 5–6 µm into the cell (Fig. 51) but, as mentioned above, this may be a result of retraction during fixation.

The cell in Fig. 45 possesses 32 rows of dikinetids. We observed 11 pairs of cilia in each row of dikinetids (Fig. 52), associated on the oral side of the row with two pairs of centrioles. In one cell an additional basal body was attached to the oral end of the 11 pairs, making it 12 (data not shown). The centrioles were situated at right angles to the first pair of axoneme-bearing basal bodies (Fig. 53), and parallel to one another (Fig. 54–56). Each centriole was associated with 3- and 1-stranded microtubular root templates (Fig. 54, 55). That the roots were short templates rather than fully formed

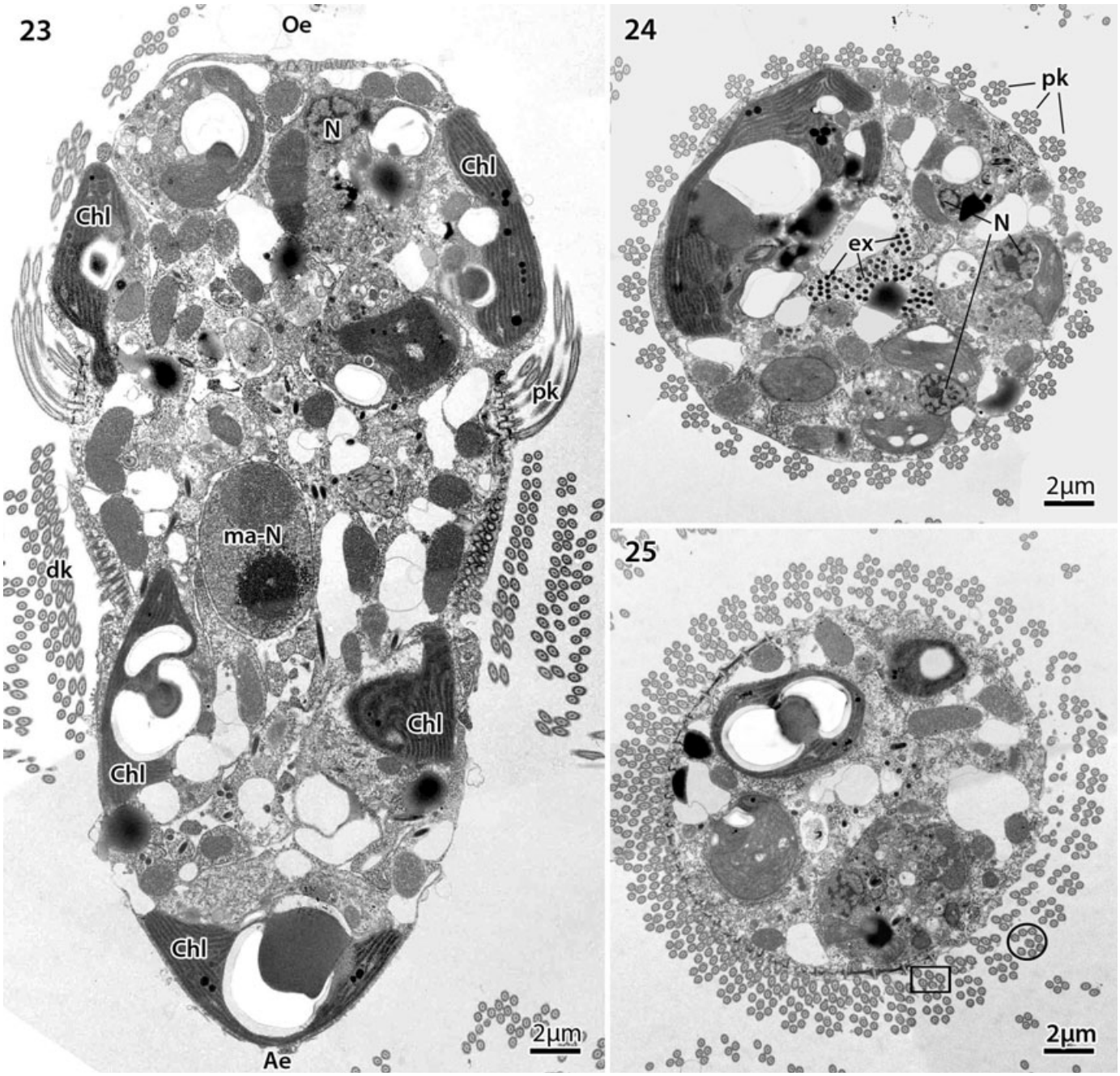

Fig. **23–25.** Transmission electron micrographs of *Mesodinium rubrum*. **23.** Longitudinal section of a cell, providing a general view: ingested prey cells with chloroplasts (Chl) and nuclei (N), dikinetids (dk), cirri (pk), and macronucleus (ma-N). Oe, oral end; Ae, aboral end. **24.** Transverse section above the girdle displaying 36 cirri (pk), each formed of eight cilia. Inside the cell many extrusomes lie in the center and three nuclei of the prey are also visible (N). **25.** Transverse section close to the base of the cirri. Short cilia found only at the base of the cell (rectangle) and cilia forming the cirri (circle) can be identified. Forty cirri are present around this cell.

roots is shown in sections as in Fig. 56, in which the quartet of centrioles was sectioned more distally and the roots had terminated.

Each cirrus base consisted of 18 basal bodies located in four rows, the rows containing 6, 5, 4, and 3 basal bodies (Fig. 57, 58). Each cirrus contained eight cilia in a 7 + 1 configuration (Fig. 43). Being somewhat swollen, the central cilium was usually distinguishable (arrowheads, Fig. 52). One-stranded microtubular roots were seen to be associated with some of the ciliary bases in the polykinetids.

Mesodinium pulex (Claparède & Lachmann). Several cells have been sectioned (Fig. 59–62, 67–78). They lacked chloroplasts but contained large numbers of vesicles of unknown function (Fig. 60), somewhat resembling nuclei in that each contained a large nucleolar-like structure. However, they were surrounded by a single membrane. The contents appeared to

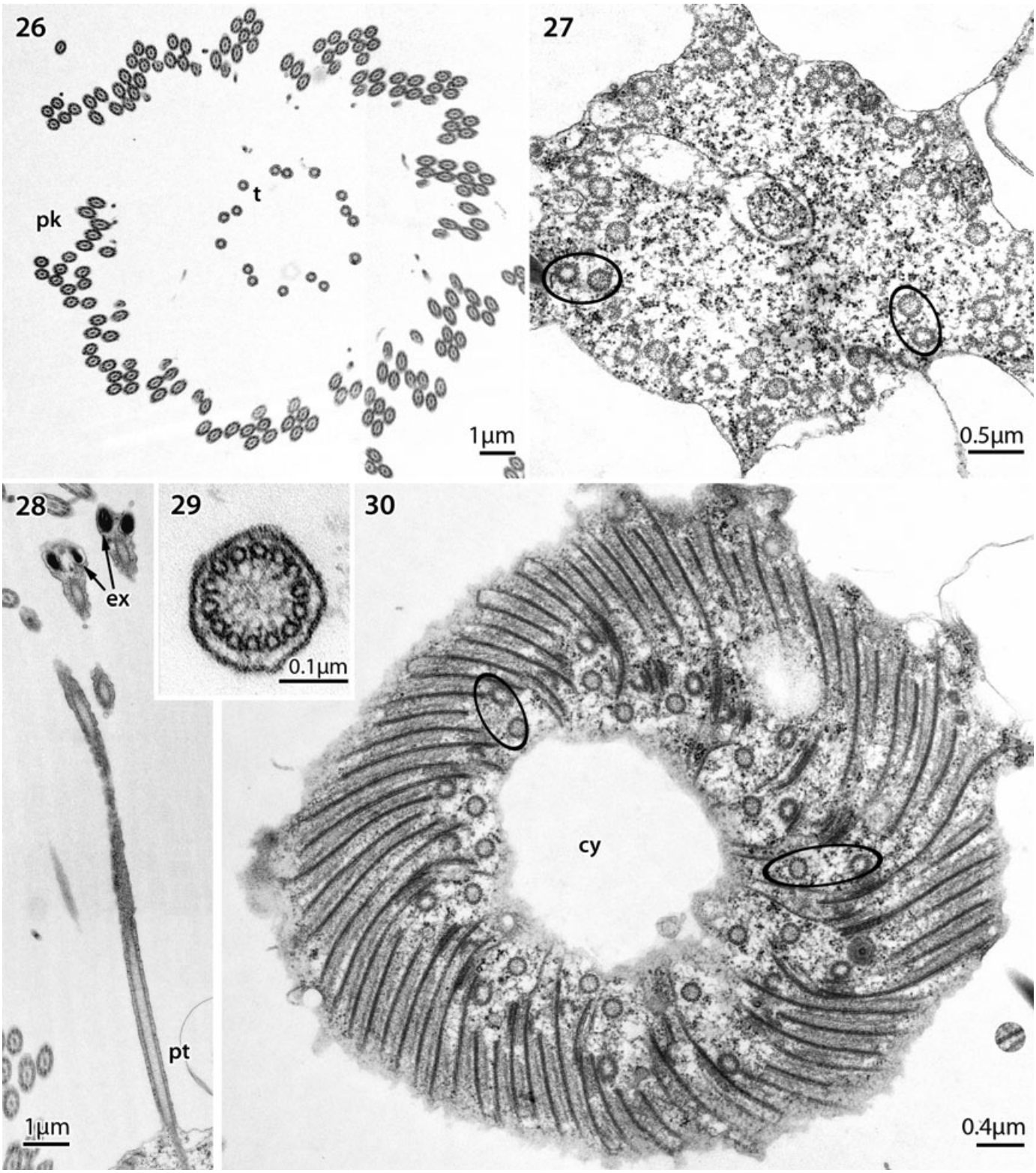

Fig. **26–30.** Transmission electron micrographs of the tentacles in *Mesodinium rubrum*. 16 tentacles (t) are visible outside the cell, forming a circle (**26**), whereas inside the cell, 16 pairs of axonemes are found (**27**, **30**). The tentacle outside the cell is supported by an axoneme of 14 microtubules (**29**) and bears extrusomes (ex) at the tip (**28**). pt: proximal part of centriole, cy: cytostome

be released to the exterior by fusion of the vesicle with the cell membrane. Cells also contained food vacuoles, in one case (from a culture) containing large parts of another cell of *M. pulex* (Fig. 59), showing that *M. pulex* may be cannibalistic, at least in culture. The number of kinetids was sometimes high (Fig. 64) but sectioning of several cells proved it to be unex-

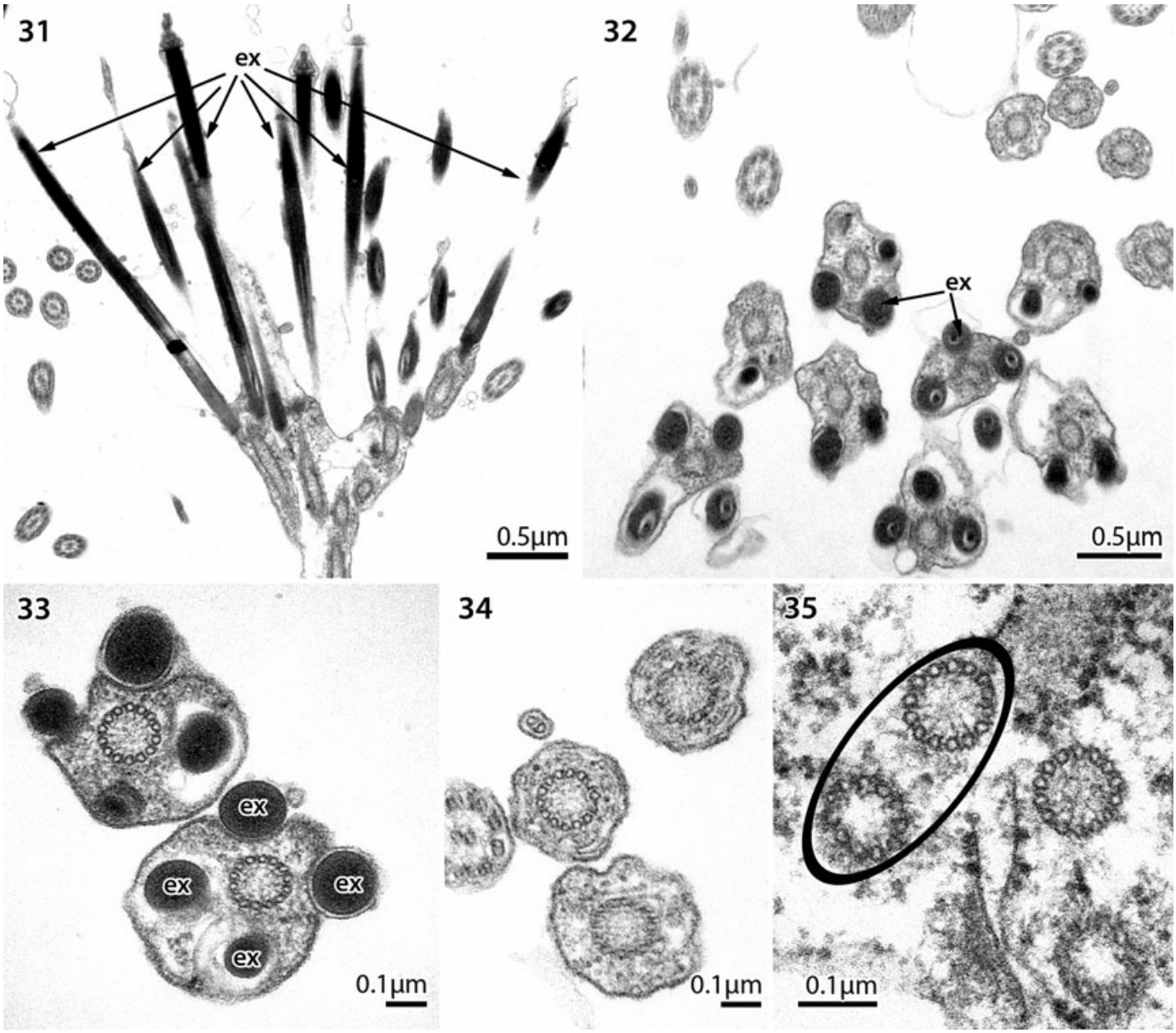

Fig. **31–35.** Transmission electron micrographs of the tentacles in *Mesodinium rubrum*. **31.** The tentacle axonemes end shortly after the extrusomes diverge (ex). **32, 33.** Transverse sections through tentacles just before the extrusomes diverge. The axoneme is formed of 14 microtubules and three to four extrusomes. **34.** Transverse section of three enlarged tentacles immediately below the area where the extrusomes diverge. **35.** Pairs of tentacle axonemes inside the cell, formed of 14 and 13 microtubules, respectively.

pectedly variable, from 33 (not shown) to 47 (Fig. 61, 62). The oral end of the cell had a conspicuous cytostome, surrounded by tentacles as well as short bulbous projections (Fig. 63, 65, 66). In SEM each tentacle was formed by a long cylindrical part that terminated distally in a pentagon of very short projections. A total of 16 tentacles was observed in sections, each tentacle supported internally by an axoneme of 23 microtubules (Fig. 69). The number of microtubules was constant from the proximal part of the tentacle at the base of the cytostome (Fig. 68) almost to the tip of the tentacle where the number started to decrease (Fig. 70, 71). The pentagon of projections was not seen in thin sections, the tentacles observed terminated without any projections being present (Fig. 72). The cell also contained a large number of extrusomes (Fig. 67, 73), often in groups (Fig. 67). Each extrusome had an opaque outer circular part surrounding an inner, less opaque part that often contained granular material. At the distal end of the tentacles, near the cytostome membrane, the contents of the extrusomes changed into a uniform gray appearance (Fig. 73). The cytostome was lined by a palisade of microtubular bands, located at right angle to the cytostome membrane (Fig. 67, 74). Each band comprised around seven microtubules and these were joined by a few additional microtubules at the cytostome membrane (Fig. 74). The cytostome gave the impression of being an area of intense activity and was filled with membranous material (Fig. 67).

Each dikinetid row comprised seven to nine dikinetids (Fig. 59). At the oral end of each dikinetid four centrioles

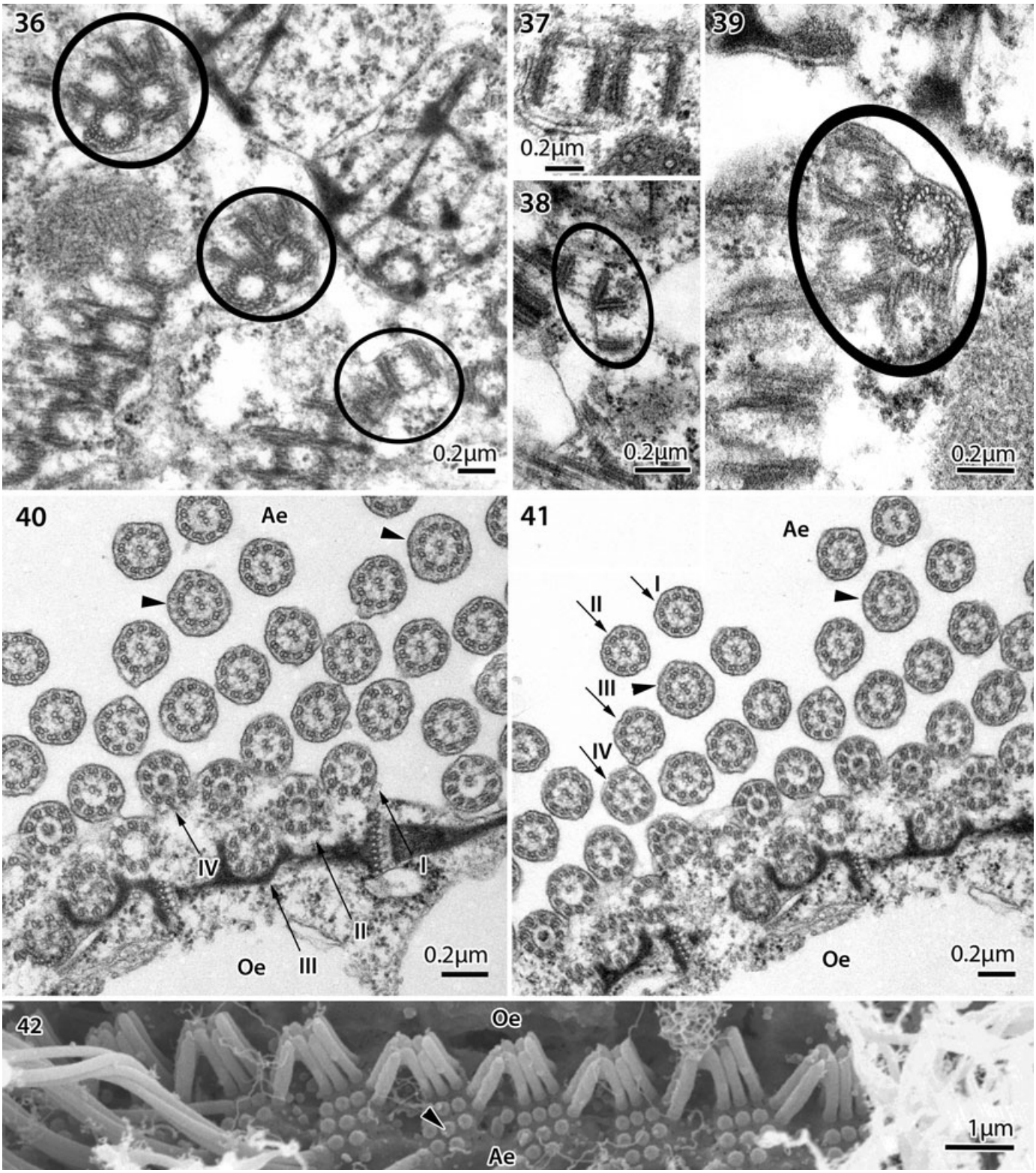

Fig. **36–42.** Transmission electron micrographs and scanning electron micrograph of *Mesodinium rubrum*. **36–39.** Two pairs of naked centrioles are located at the oral end of each dikinetid row (36). Centrioles of each pair are positioned at ~ 60° to one another (38) while the centrioles within each pair are almost parallel (37). The dikinetids have been sectioned in the lower left part of the figure, while the fibrous structures on the upper right in the figure interconnect the cirral basal bodies. **40–42.** Each cirrus is formed from 16 basal bodies, arranged in four rows of 5, 5, 4, and 2 basal bodies (I, II, III, IV). Eight of the 16 form the cirri while the other eight terminate shortly after emerging from the cell (42). Arrowheads: central cilium in the cirri.

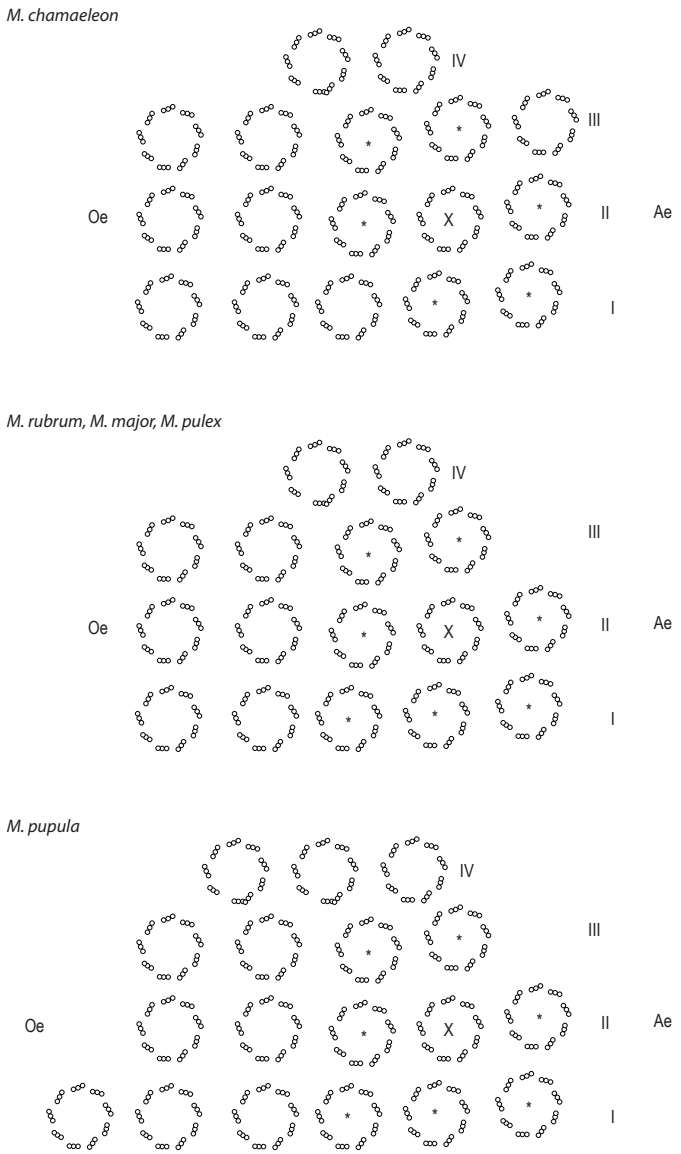

Fig. **43.** Diagrammatic representation of cirri in *Mesodinium* species. In *M. chamaeleon* (top row) each cirrus is formed from 17 basal bodies, arranged in four rows of 5, 5, 5, and 2 basal bodies. The oral end of the cell (Oe) is toward the left in the figure, the aboral end (Ae) toward the right. Whereas nine of the basal bodies extend into short (~ 1 μm long) cilia of unknown function, the remaining eight cilia form the cirrus proper, the cilia arranged in a 6 + 1 configuration. The seven basal bodies indicated with asterisks form the peripheral cilia of each cirrus, while the basal body indicated with the "x" forms the central cilium. *M. rubrum*, *M. major* and *M. pulex* (middle row) lack one basal body in row III, and the middle basal body in row I participates in forming the emergent part of the cirrus, resulting in a 7 + 1 configuration. *Mesodinium pupula* also lacks a basal body in row III but possesses an additional one in row 1 and row IV. The emergent part of each cirrus is formed by eight cilia in a 7 + 1 configuration.

were arranged nearly parallel to one another and nearly perpendicular to the first pairs of dikinetids (Fig. 75).

Each cirrus was composed of 7 + 1 cilia, which emerged from a basal system of four rows of basal bodies, formed by 5, 5, 4, and 2 basal bodies (Fig. 43). The central cilium of each cirrus was somewhat thicker than the rest, and thus readily distinguishable (Fig. 76–78). Two of the peripheral cilia in each 7 + 1 cirrus were shorter than the others, and the cirri thus comprised six cilia for most of its length (5 + 1) (Fig. 77). An unusual feature, not observed in other species, was the presence of opaque bars in a cilium in each cirrus (i.e. the cilium in row 3, position 3). Three bars extended near one of the peripheral doublets in the cilium and another opaque mass of material from another doublet (Fig. 76). The bars supported short wings, and the former was joined by a similar 3-barred wing on the adjacent cilium in row 3, position 4 (Fig. 76). The latter cilium was one of the short cilia and soon terminated: fully present in Fig. 76, but only as a shadow on two cilia in Fig. 78.

To simplify comparison of the five species, an illustrated key was constructed to the marine *Mesodinium* species studied in this article. The drawings (Fig. 79–84) are schemes based on light microscopy (Table 1) and ultrastructural (Table 2) data.

1. Cells without chloroplasts..... 2
Cells with chloroplasts..... 3
2. Oral end typically conical, aboral end spherical, cells 25–28 μm long and 16–25 μm wide, found both planktonic and benthic..... *M. pulex*
Pear-shaped body with equally sized hemispheres, cells 26–30 μm long and 19–27 μm wide, benthic..... *M. pupula*
3. Cells benthic with usually green plastids; hemispheres rounded, the oral hemisphere slightly shorter than the aboral one, cells 19–25 μm long and 13–17 μm wide..... *M. chamaeleon*
Cells planktonic, always containing reddish plastids..... 4
4. Oral hemisphere rounded, aboral end conical, cells 25–35 μm long and 16–25 μm wide..... *M. rubrum*
Both hemispheres hemispherical, or oral end slightly flattened, cells 40–55 μm long and 35–50 μm wide, oral end sometimes changing into so-called Medusa-form ..... *M. major*

Phylogeny. The phylogenetic analysis based on the SSU rDNA alignment of 972 bp allowed identification of three well-supported clades (Fig. 85). The first and second clades contained sequences closely related to sequences of *M. pulex* and *M. pupula,* respectively. The third clade contained all the mixotrophic species and could in turn be divided into two subclades. The first group starting from the top is formed by sequences closely related to the sequence of *M. chamaeleon*. The second is formed by sequences of all the strains of *M. rubrum*, *M. major* n. sp., and other closely related environmental sequences that probably represent other species or variants containing endosymbionts related to or originating from cryptophytes belonging to the *Teleaulax/Plagioselmis/Geminigera clade*. The large radiation within this subclade is unresolved, yet none of the isolates grown in culture had identical sequences except for the Japanese and Korean isolates.

The rDNA block alignment consisted of 2,131 bp that cover most of the SSU rDNA gene as well as the ITS region and the beginning of the LSU rDNA. The phylogenetic analysis based on this alignment yielded the tree topology that divided the six species of marine *Mesodinium* into two clear clades with high posterior probabilities and bootstrap values (Fig. 86). The first is formed by the heterotrophic species *M. pupula* and *M. pulex*. The second clade is formed by the mixotrophic species *M. chamaeleon*, *M. major* n. sp., and *M. rubrum*, originating from Denmark and Antarctica.

The molecular phylogeny of the phototrophic marine isolates based on the ITS block alignment generated a tree in which five clades can be identified with statistical support

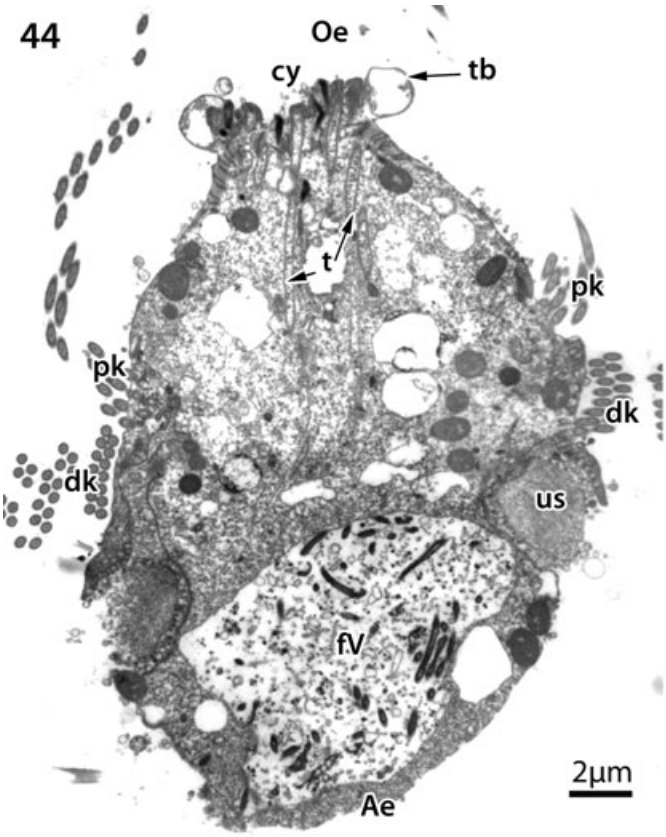

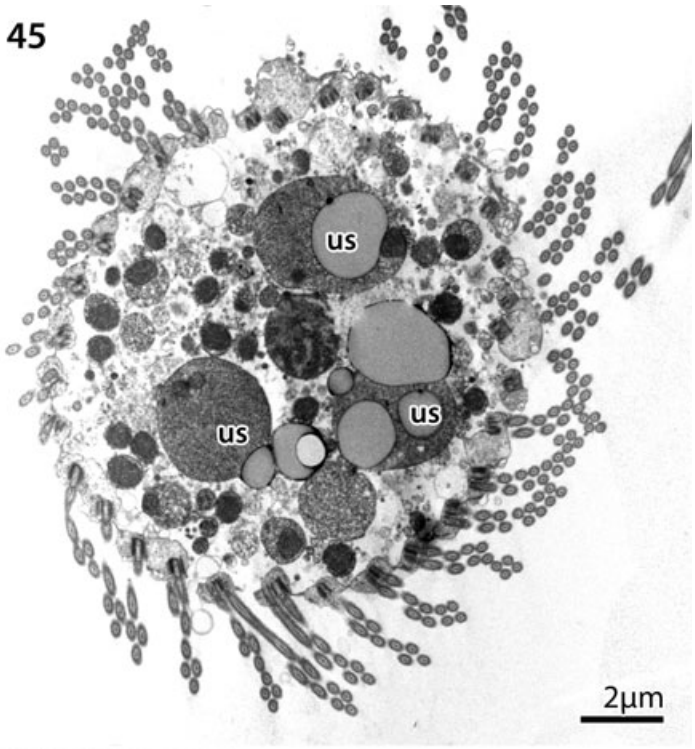

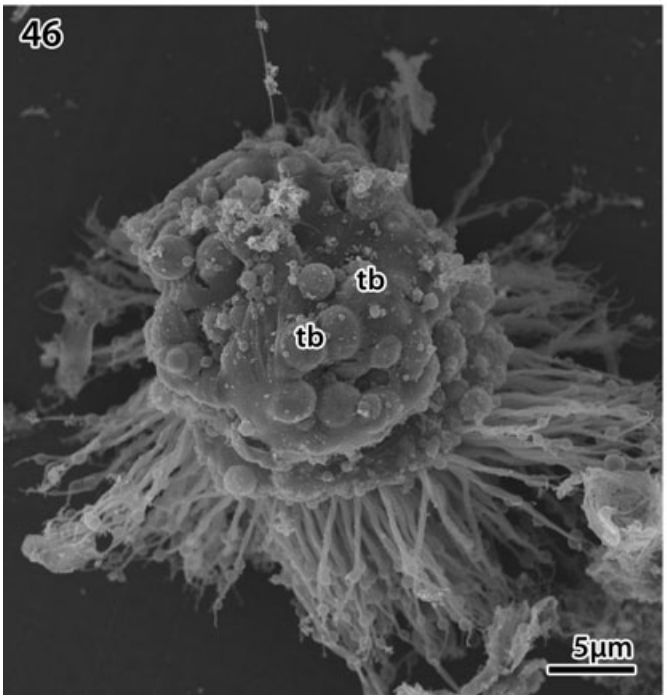

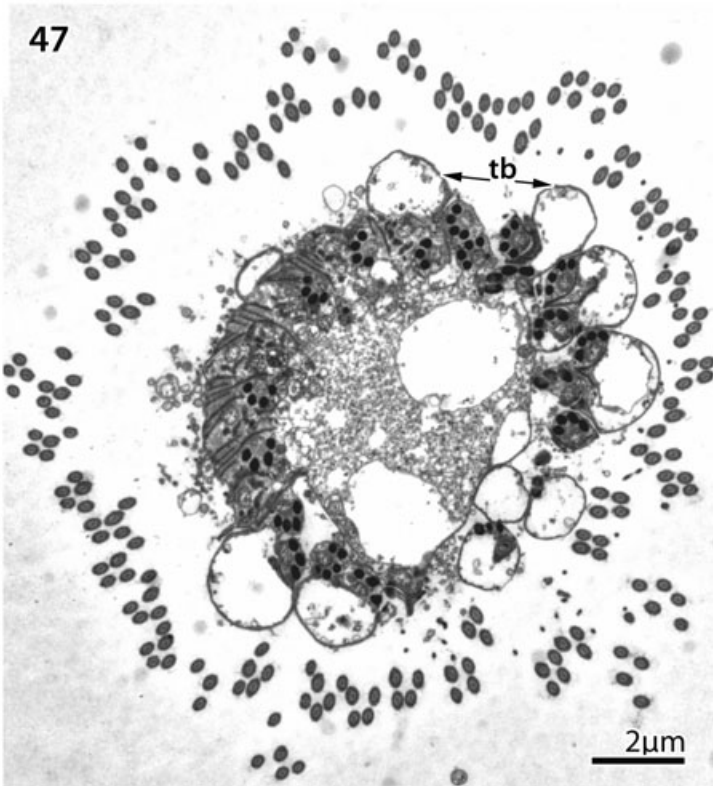

Fig. **44–47.** Transmission electron micrographs and scanning electron micrograph of *Mesodinium pupula*. **44.** Longitudinal section of the cell, providing a general view: cytostome (cy), tentacles within the cell (t), bulge containing tentacle axoneme (tb), dikinetids (dk), cirri (pk), and food vacuole (fV). Unidentified opaque vesicules are also present (us). Oe, oral end; Ae, aboral end. **45.** Transverse section across the dikinetid rows showing several grayish vesicles (us) within the cell. **46.** Scanning electron micrograph of cell in apical view. No tentacles are seen outside the cell but the oral end is covered with tentacular bulges (tb). **47.** Transverse section across the cytostome area. The bulges (tb) contain tentacle axonemes, each bulge containing three to four extrusomes. Compare with Fig. **48–51**.

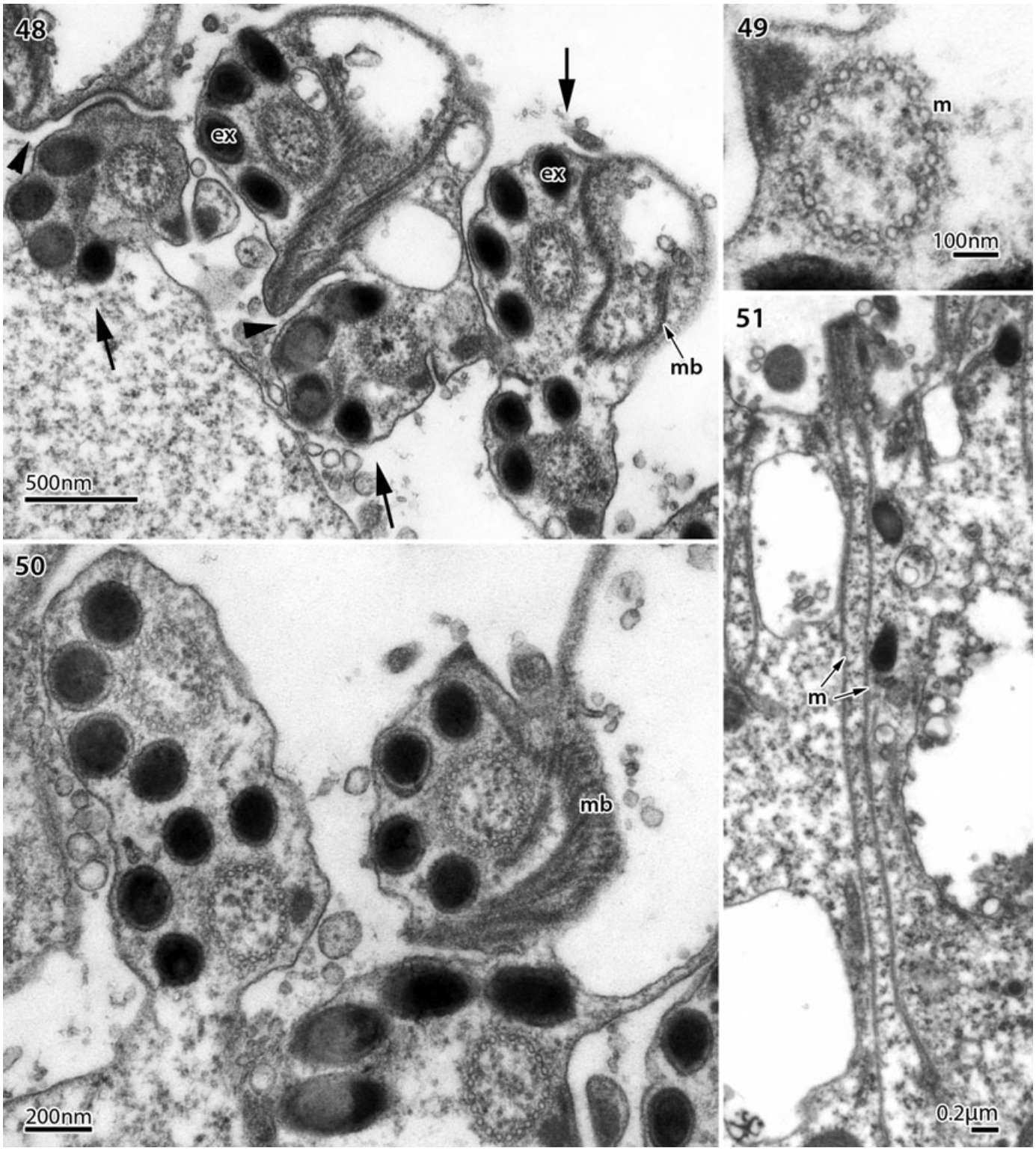

Fig. **48–51.** Transmission electron micrographs of the tentacles in *Mesodinium pupula*. **48.** Oblique section across three tentacle swellings. Each swelling (arrows) is formed of two axonemes accompanied by four extrusomes (ex). Both axonemes are united in the same base proximally (on the right) while they form two separate entities distally (on the left). Arrowheads indicate forming or full gaps between the two parts. **49.** The axoneme within each tentacle is formed of 23 microtubules. **50.** A band of microtubules (mb) is present between the two parts of the tentacle bulge and these eventually extend into the outermost tentacle. **51.** Longitudinal section of the oral end showing tentacle axonemes extended for 5–6 µm into the cell. m: microtubules.

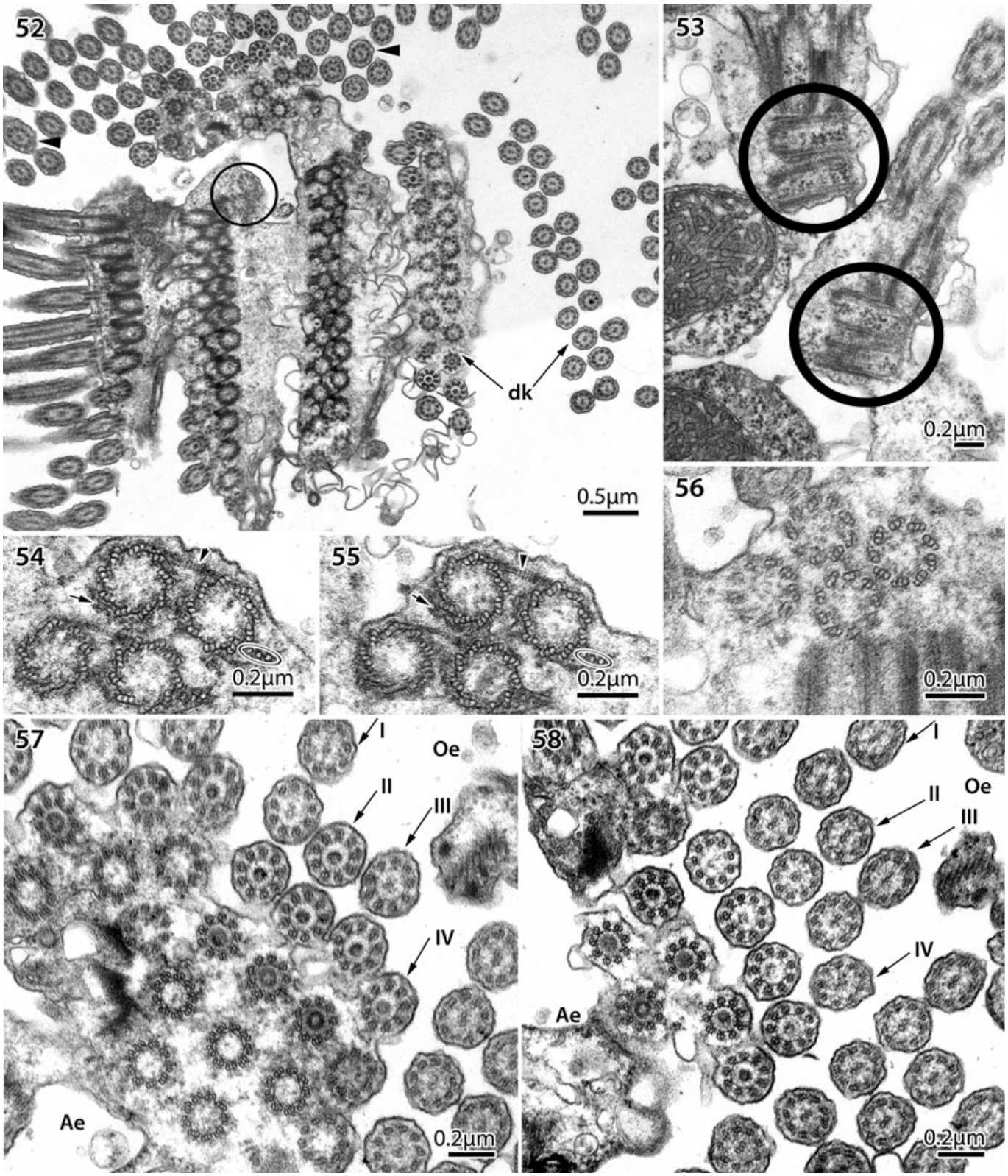

Fig. **52–58.** Transmission electron micrographs of *Mesodinium pupula*. **52.** Rows of 11 dikinetids (dk). One pair of naked centrioles is visible at the top of the dikinetid row (circle). **53.** Pair of centrioles in longitudinal section (circles) at right angles to the first pair of axoneme-bearing basal bodies. **54–56.** The four centrioles are parallel to one another and associated with 3- and 1-stranded microtubular root templates (arrow), which have terminated in Fig. 56. Arrowheads indicate connecting fiber between two centrioles. **57, 58.** Each cirrus is formed from 18 basal bodies, arranged in four rows of 6, 5, 4, and 3 basal bodies. Eight of the 18 form the cirri while 10 terminate shortly after emerging from the cell. Oe, oral end; Ae, aboral end.

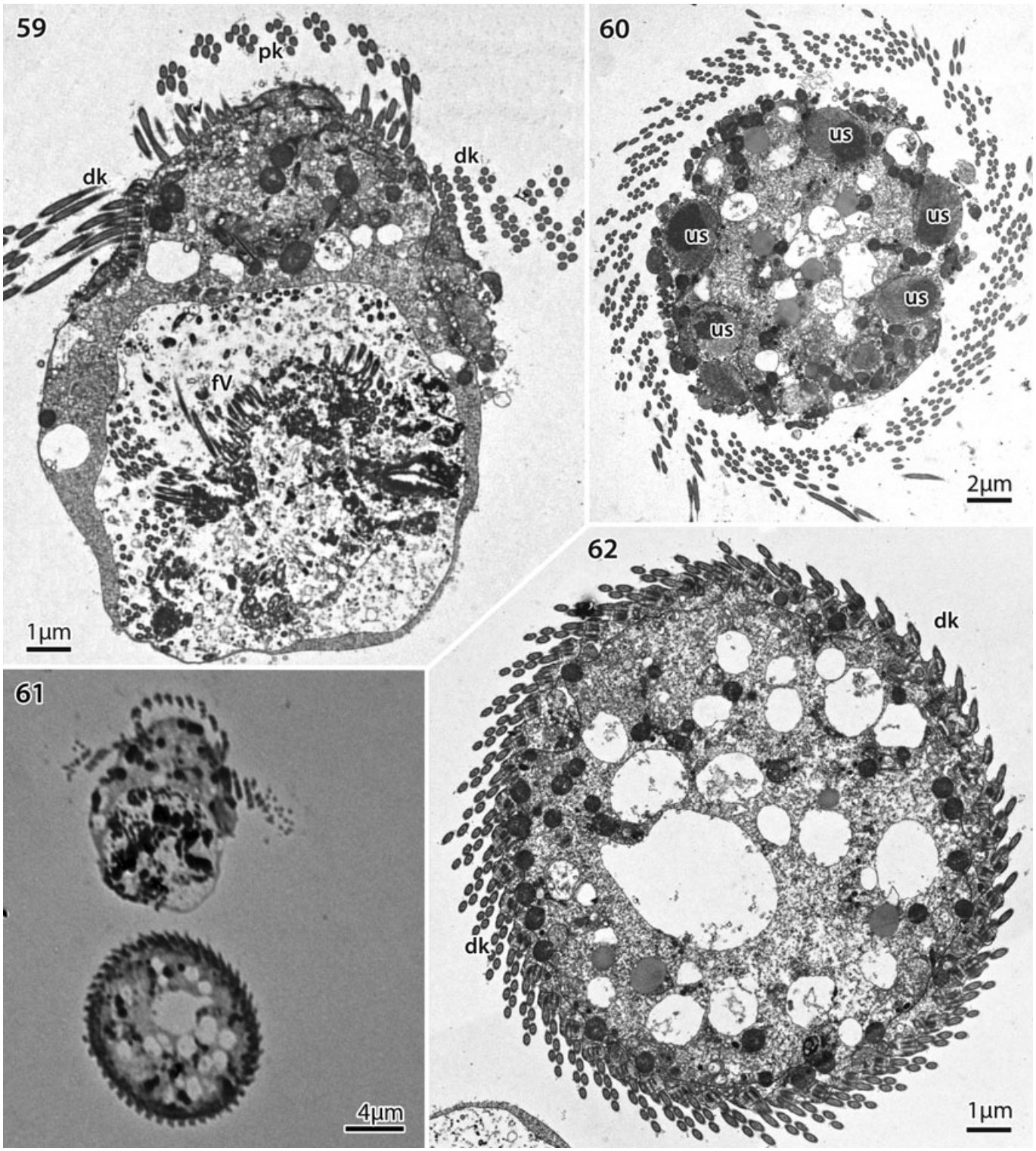

Fig. **59–62.** Cells within the plastic block prior to sectioning, and transmission electron micrographs of *Mesodinium pulex*. **59.** Longitudinal section of the cell, providing a general view: dikinetids (dk), cirri (pk), and food vacuole (fV). Note the *M. pulex* cell within the food vacuole. **60.** Transverse section across the dikinetids. Many unidentified vesicles (us) are visible. **61.** The cells within the plastic block, before Fig. 59 and 62 were taken. **62.** Transverse section with 47 rows of dikinetids.

(Fig. 87). Clades were named according to Herfort et al. (2011) as variants A, B, C + E, D, and a new variant was identified in the present study and named variant F. Containing only one sequence, variant F corresponds to the Danish isolate of *M. rubrum*. *Mesodinium major* and the *M. rubrum* CCMP 2563 belong to clade D and A, respectively.

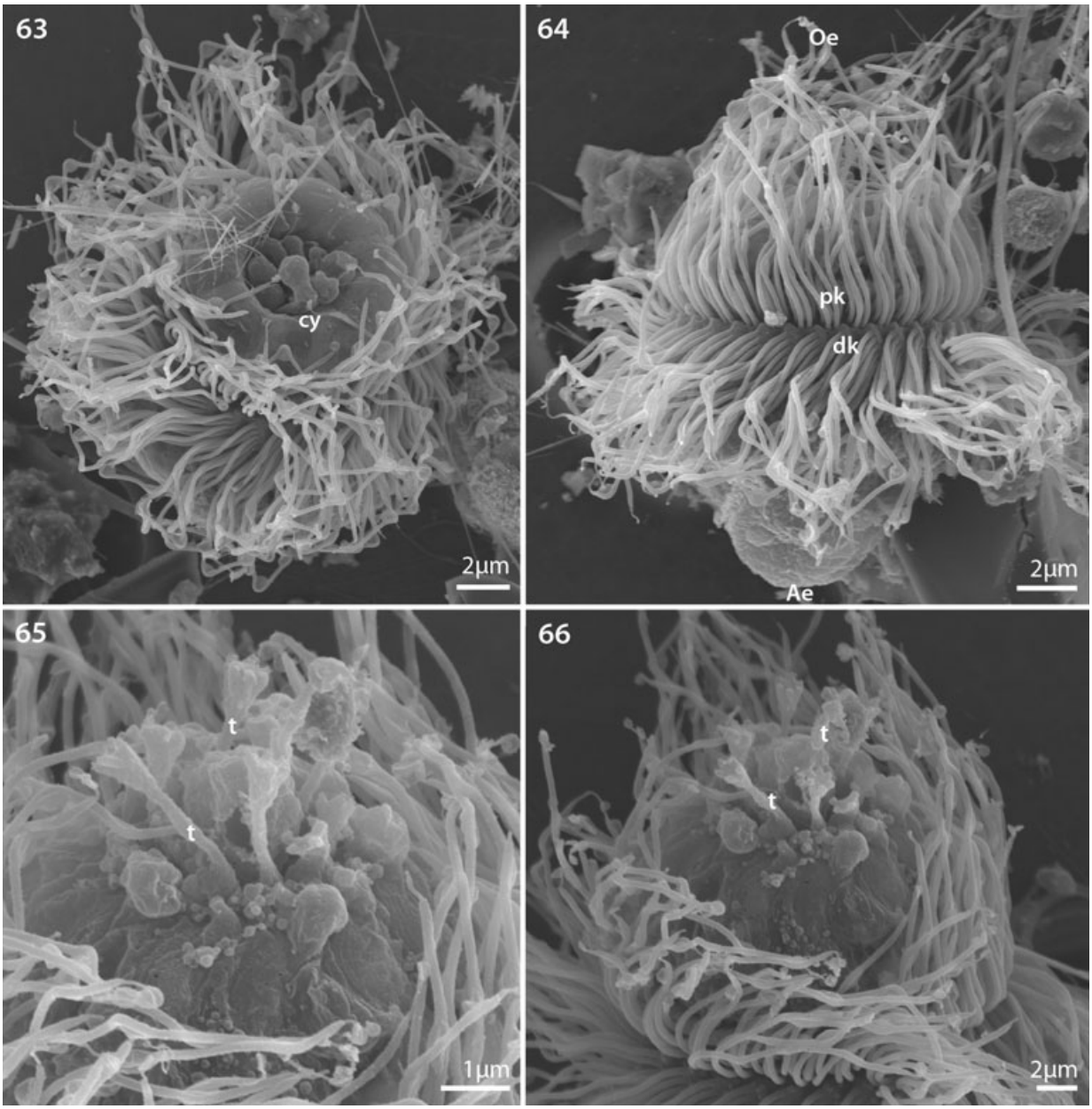

Fig. **63–66.** Scanning electron micrographs of *Mesodinium pulex*. **63.** Apical view of the cytostome (cy) with small bulges. **64.** Cell viewed from the side where the belt of cirri (pk) and rows of dikinetids (dk) are arranged in alternation. **65**, **66.** Tentacles (t) of cell emerging from the cytostome. Distally each tentacle extends into a short concave pentagon. Small bulges can be seen at the base of the tentacles.

Chloroplast identification. Sequences of the chloroplast fragment containing the partial 16S rDNA, tRNA-Ile gene, the tRNA-Ala gene, Intergenic Transcribed Spacer (ITS), the partial 23S rDNA, and the nucleomorph LSU rDNA were only obtained for *M. major* and were given the GenBank accession number (JQ347803) and (JQ347802), respectively. Both sequences are identical to *T. amphioxeia* (GQ396296 and GQ396273) and *M. rubrum* (GQ396295 and GQ36272).

DISCUSSION

Generic name. Jankowski (2007) argued that the main difference between *Myrionecta* and *Mesodinium* is a different arrangement of the kinetids forming the ciliary belts. This assumption was probably based on the early work on *M. pupula* (Dragesco 1963), *M. pulex* (Borror 1972), and *M. rubrum* (Taylor et al. 1971) where the heterotrophic species are said to have kinetids arranged in lines of five at the base of the cirri, versus the cluster arrangement of kinetids found in *M. rubrum*. Subsequently, a key to the genera of the family Mesodiniidae was constructed by Krainer and Foissner (1990) based on a series of studies (Borror 1972; Fauré-Fremiet 1924; Grain et al. 1982; Jankowski 1976; Lindholm 1985; Tamar 1987) and generally accepted by the scientific community. The ultrastructural results obtained in the present study show no major difference in the somatic ciliary arrangements between the five species examined; all are constructed after a common pattern. The number of dikinetids differs and so does the number of cilia forming the cirri, but the arrangement per se does not. The arguments for dividing the species into different genera

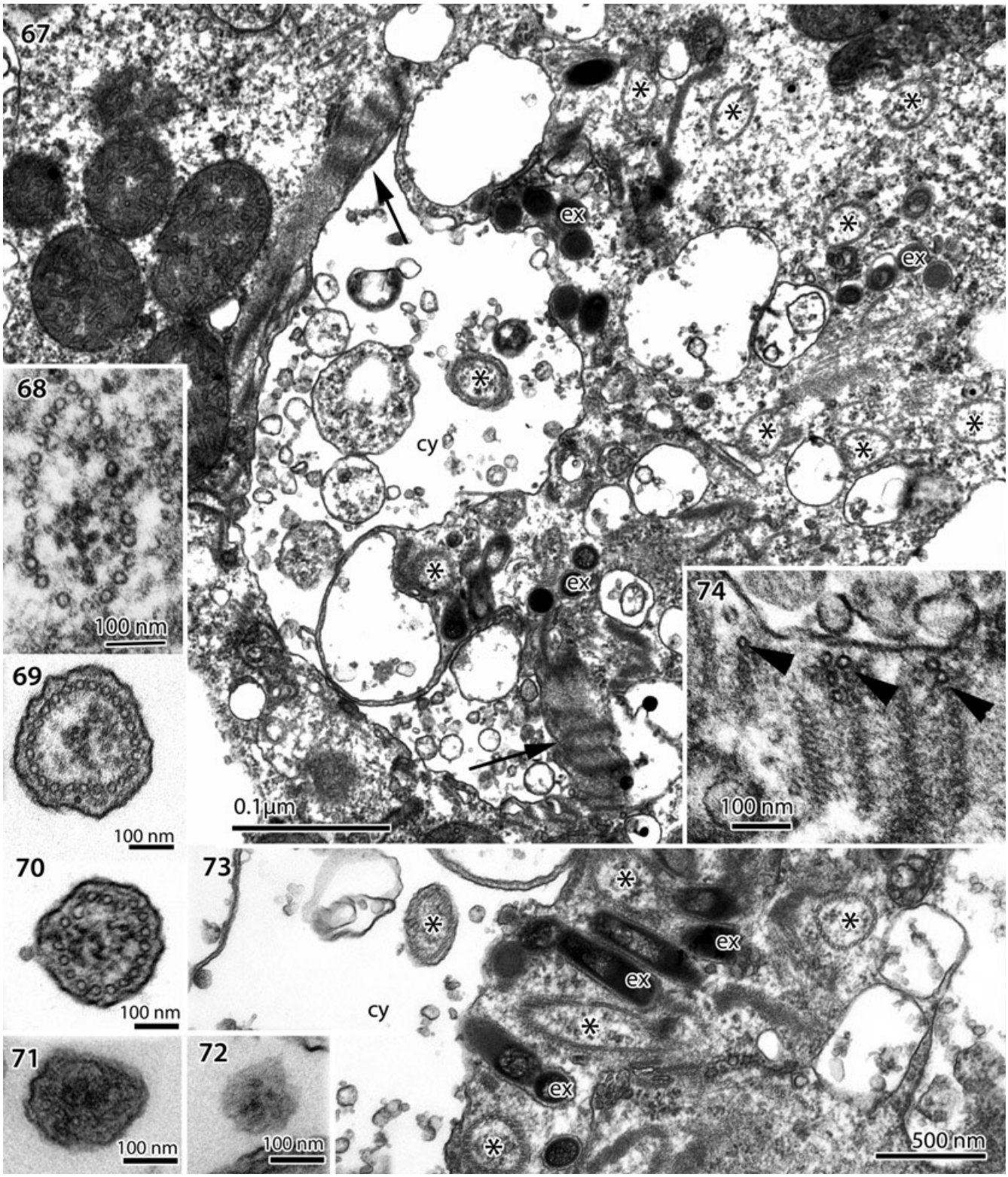

Fig. **67–74.** Transmission electron micrographs of *Mesodinium pulex*. **67.** Transverse section through the cytostome (cy) showing the tentacle axoneme (asterisk), the extrusomes (ex), and the palisade of microtubular bands, located at right angle to the cytostome membrane (arrows). **68–72.** Tentacle cross sections. Twenty-three microtubules form the axoneme within the cell (68). The number remains unchanged at the cytostome level (68), almost to the tip of the tentacle (69), but deceases near the tip (70). In Fig. 71 a few microtubules are still visible, while Fig. 72 is the last section of the tentacle. **73.** The extrusomes (ex) lay within the cell and are distributed between the axonemes of the tentacles (asterisks). One tentacle is visible in the cytostome. **74.** Palisade of microtubular bands, located at right angles to the cytostome membrane, and joined along the cytostome membrane by a few additional microtubules.

Table **2.** Summary of the ultrastructure (TEM) of the five *Mesodinium* species.

	Tentacles under the surface of the cytostome	Axonemes in the tentacle outside the cell	Cirri[a]	No of cilia at the cirral base[a]	Cilia in the cirri[a]	No of dikinetids[b]
M. pupula	16 pairs	23	~ 32	18 (6,5,4,3)	7 + 1	~ 11
M. pulex	16 pairs	23	~ 32 to 47	16 (5,5,4,2)	7 + 1	~ 9
M. chamaeleon	10 pairs	13	~ 34	17 (5,5,5,2)	6 + 1	~ 11
M. rubrum	16 pairs	14	~ 36 to 40	16 (5,5,4,2)	7 + 1	~ 16
M. major	–	14	~ 74	16 (5,5,4,2)	7 + 1	~ 24 to 25

[a]Numbers confirmed by light microscopy counts (n = 10).
[b]Numbers confirmed by SEM micrographs (n = 4).

because of different construction of the kinetids, therefore do not hold.

It could be argued that a similar somatic kinetid pattern is found in different genera of ciliates, and other criteria are used to segregate them. Significant morphological differences exist between the five species, however. For example, one of the most diverse features is the construction of the tentacles as discussed in detail below. They vary considerably, perhaps reflecting the different feeding modes. Based on this character only, it could be argued that the marine *Mesodinium* should be divided into two or three genera. One genus might include the heterotrophic species *M. pulex* and *M. pupula* with their 23-microtubule tentacles, the second might comprise the photosynthetic *M. rubrum* and *M. major* with their 14/11 system of tentacles and the third apparently mixotrophic *M. chamaeleon* with its 13/11 tentacles. A case could be made for merging the latter two. Yet, based on the construction of the cirral bases *M. pupula* stands out in having 18 basal bodies in each cirral base, *M. pulex* has 16, and *M. chamaeleon*, *M. rubrum* and *M. major* n. sp. have 17. Then again, based on the number of cilia forming each cirrus, *M. chamaeleon* stands out with its 6 + 1 system, while all the other species have the same 7 + 1 type. Cell division, although not known in detail, appears to be similar in the species studied by us and the account of the freshwater species *M. acarus* (Tamar 1987). However, these morphological differences fail to consistently segregate the five marine species into the same different genera and the lack of ultrastructural data on freshwater species, including the type species *M. acarus* J. Stein, prevents a sound evaluation of the morphological differences.

The genetic data also show high similarity between different clades. The distinctive deletions and substitution changes (i.e. indels) in the SSU rDNA found to set the genus *Mesodinium* apart from other litostomatean ciliates (Johnson et al. 2004; Strüder-Kypke et al. 2006) were present in all sequences, whether from freshwater or marine species. On the other hand, freshwater species seem to have a different molecular signature allowing the LG-D primer set to be freshwater specific (Bass et al. 2009). Although the molecular data indicate that the freshwater and the marine species constitute separate groups, the estimates of evolutionary divergence over sequence pairs between marine clades are within the same range as estimates of evolutionary divergence over sequence pairs between marine and freshwater clades (Table 3). A separation of the marine and the freshwater species into two different genera based on SSU rDNA sequences would lead to the formation of three new genera in the marine. Yet, in the absence of ultrastructural studies of any freshwater species, which includes the type species, *M. acarus*, and since the relative distances between clades are so small, it is our opinion that they all be assigned to the same genus—*Mesodinium*. Presently some species names are used for both marine and freshwater taxa, and the validity of this also needs confirmation.

Mesodinium pupula. Although the data collected in this study generally agree with both previous descriptions of *M. pupula* (Dragesco 1963; Kahl 1935), the arrangements of the kinetids forming the cirri are very different. Not only were the short cilia at the base of the cirri overlooked in the more detailed description by Dragesco (1963), but the arrangement and number of cilia forming the cirri are incorrect. The cirri are formed of seven not five cilia and are not arranged in a row of 5 but in a cluster of 18, resembling the cluster of 16 in *M. rubrum* (Grain et al. 1982). Other characteristics, such as ecology, size and shape of the cell, the number of cirri, and the number of dikinetids per row matched our data.

Mesodinium pulex. The isolate from the U.S. examined by us agrees well with *M. pulex* from Danish waters. The number of cirri (i.e. 32–49) is impressive considering the small size of the cell and corresponds to the range obtained in previous studies (Borror 1972; Tamar 1992). The plasticity of the oral end and the conspicuous cytostome are important species characteristics. The number of tentacles surrounding the cytostome also agrees with previous studies. One of the most striking features of this species is that the tips of the tentacles do not support extrusomes. This finding disagrees with Borror (1972) where two and five branches were enumerated, respectively. Tamar (1992) later described the cone-shaped distal parts of the tentacles in an article dedicated to *M. pulex*, where it was mentioned as resembling a suction cup or funnel.

The photosynthetic endosymbiont-bearing *Mesodinium*: species or species complex? Despite having a somewhat similar morphology and by possessing plastids of the same origin, *M. rubrum* and *M. major* n. sp. differ markedly in cell size and ecology. To begin, both species occur in the water column throughout the year but may be identified by a trained eye. However, they thrive at different times of the year. *Mesodinium rubrum* is abundant in the summer and early autumn whereas *M. major* is found mainly in the winter and early spring in Danish waters. Another striking difference between the two species is the ability of *M. major* to develop into a Medusa-form, which has never been recorded in strains of *M. rubrum*, despite changes in experimental conditions. Last but not least, *M. rubrum* can be maintained in culture whereas so far, *M. major* cannot, regardless of the common nature of their plastids, and indicating a physiological difference between them. Therefore, we consider that they are two different species.

In the literature they are both referred to as *M. rubrum*, except by Leegaard (1920), who separated the two size groups into *M. rubrum* forma *minor* and *M. rubrum* forma *major*. Lohmann (1908) original description of *M. rubrum* as *Halteria rubra* is based on several species, most likely three: the heterotrophic *M. pulex*, and at least two of the red phototrophic species. Lohmann (1908) discriminated among the three types of *H. rubra* cells. The first type was colorless and 10–18 μm

Fig. **75–78.** Transmission electron micrographs of *Mesodinium pulex*. **75.** Pairs of centrioles in longitudinal section (circles) at right angles to the first pair of axoneme-bearing basal bodies. **76, 77.** The slightly thicker central cilium of each cirrus (arrowhead) is surrounded by seven cilia at the base. Yet only five fully develop and together with the central cilium form the cirri (77). **78.** Each cirrus is formed from 16 basal bodies, arranged in four rows of 5, 5, 4, and 2 basal bodies. Oe, oral end; Ae, aboral end.

long, with a morphology similar to *M. pulex*, including a conical oral end with a cytostome, and a rounded aboral end. The second type was very similar but slightly larger and contained one or two small plastids. The third type was 20–50 µm long with up to 100 plastids, and the cells had a more rounded oral end in which a cytostome could not be seen. The first two

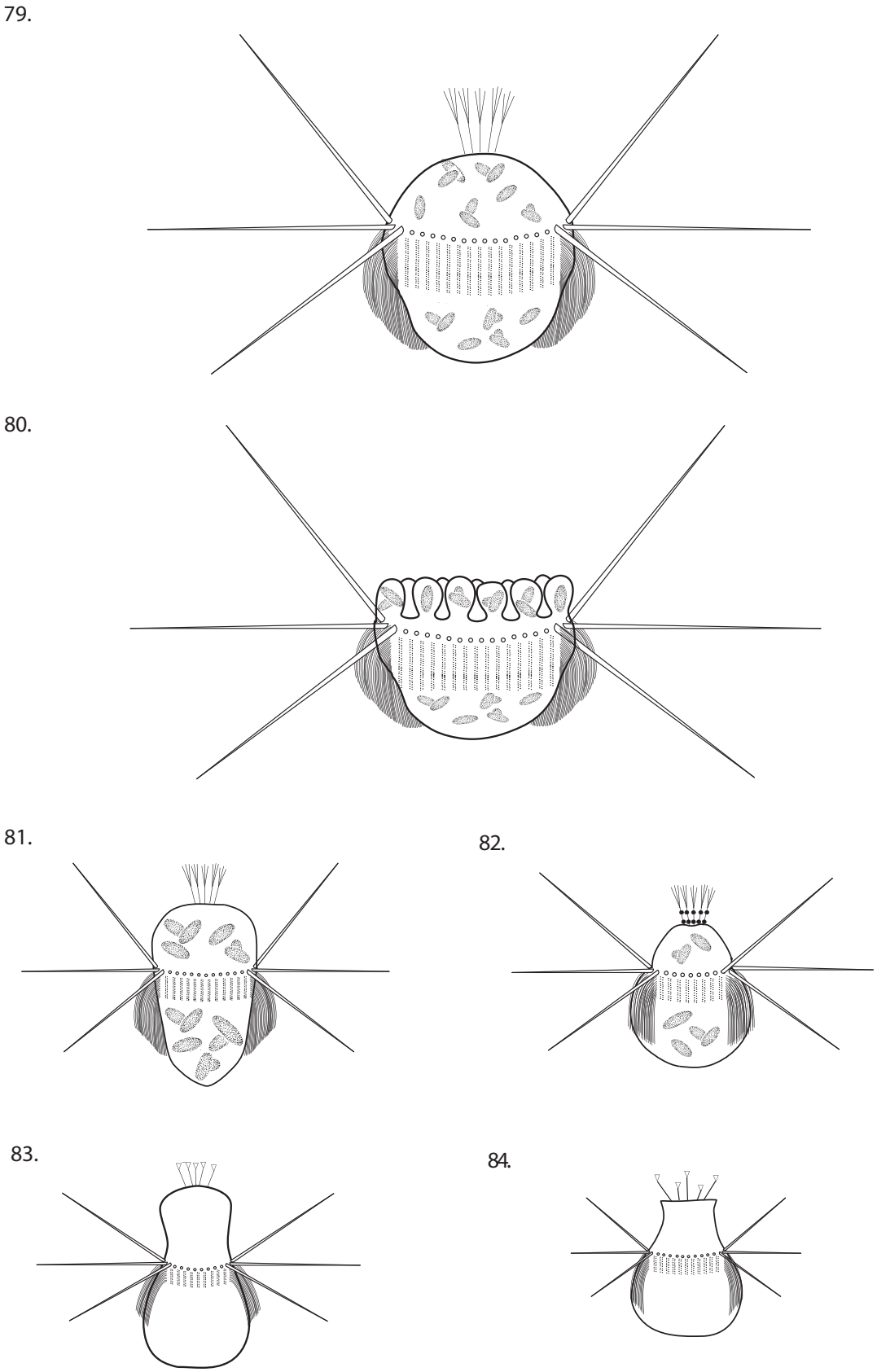

Fig. **79–84.** Schematic drawing of the five *Mesodinium* species. **79.** *Mesodinium major*. **80.** *Mesodinium major* Medusa-form. **81.** *Mesodinium rubrum*. **82.** *Mesodinium chamaeleon*. **83.** *Mesodinium pupula*. **84.** *Mesodinium pulex*.

Table **3.** Estimates of evolutionary divergence over sequence pairs between clades.

	Clade 1	Clade 2	Clade 3	Clade 4	Freshwater outrgroup
Clade 1	0				
Clade 2	0.060	0			
Clade 3	0.080	0.075	0		
Clade 4	0.074	0.072	0.026	0	
Freshwater outgroup	0.041	0.046	0.074	0.066	0

The number of base differences per site from averaging over all sequence pairs between groups is shown. The analysis involved 64 nucleotide sequences. All positions containing gaps and missing data were eliminated. There were a total of 939 positions in the final dataset. Evolutionary analyses were conducted in MEGA5 (Tamura, K., Dudley, J., Nei, M. & Kumar, S. 2007. MEGA4: Molecular Evolutionary Genetics Analysis (MEGA) software version 4.0. *Mol. Biol. Evol.*, **24**:1596–1599.)

types appear to belong to *M. pulex* and represent the variation observed within populations in size and feeding state. The first or second plastids may be food vacuoles. The third type appears to include both the two phototrophic *Mesodinium* species studied herein, if not more. Considering the concomitant occurrences of the red phototrophic species in our sampling area, which is geographically close to Kiel Bay where Lohmann (1908) worked, it appears likely that both species were present in his spring and autumn samples. To avoid additional taxonomic confusion, we decided to define the smaller variety as *M. rubrum* while the larger variety has been named *M. major* n. sp., using the variety name of Leegaard (1920). Most studies on *Mesodinium* deal with the smaller variety, and the species name generally used is *rubrum*.

Based on ITS block phylogeny, more species or variants may be found. Herfort et al. (2011) identified five *M. rubrum* variants in the Washington River, USA, based on environmental samples. Variant B was responsible for recurrent summer blooms. All variants agree in the origin of the plastids, which belong to the cryptophyte *Teleaulax/Plagioselmis/Geminigera* clade. When compared with our sequences, the Danish type of *M. rubrum* appeared to be a newly discovered genetic variant while *M. major* n. sp. corresponds to the already identified variant D. Whether or not all the variants recorded in Herfort et al. (2011) represent different species with different morphologies and ecologies is still to be investigated. Herfort et al. (2011) observed no morphological differences under the light microscope when single cells were isolated to perform single-cell PCR amplification to compare with the environmental sequences obtained. Two retrieved sequences (GenBank accession number HQ227992 and HQ227993) belonged to variant B while two others (GenBank accession number HQ227991 and HQ227994) belonged to variant A and C, respectively. This suggests that no major morphological difference exists between variants A, B, and C.

Tentacles. Tentacle structure of *Mesodinium* species seems to be a reflection of their feeding strategies and the genus can be divided according to this criterion. One type of tentacle occurs in the mixotrophic species *M. chamaeleon, M. rubrum*, and *M. major* n. sp. while a second type was found in the heterotrophic species *M. pulex* and *M. pupula*. The "mixotrophic" type of tentacle was first described by Lindholm et al. (1988), based on material from the Baltic. They found 14 microtubules in the tentacles, and 11–14 within the cell. The lower number within the cell was interpreted as representing the base of the tentacles. Our studies have not confirmed this explanation. Rather, we found pairs of tentacle axonemes within the cell, comprising 11 and 14 microtubules. The latter extended as 14-microtubule axonemes in the tentacles, whereas the 11-microtubule axoneme remained within the cell. Two such pairs of axonemes are also visible in Lindholm et al. (1988, Fig. 17), separated by a 12-microtubule axoneme. In *M. chamaeleon* we occasionally saw 12-microtubule axonemes instead of the 13- and 11-microtubules axonemes (Moestrup et al. 2012), but we have no explanation for this variation in number. At the proximal end of the axoneme, at a considerable distance into the cell, the number of microtubules decreases rapidly and the axoneme terminates. Lindholm et al. (1988) mention bifurcation of the distal part of the tentacles in *M. rubrum*. In the light microscope the distal part often appears to be bifurcate. However, when studied in the SEM and TEM, the number of branches, which hold extrusomes, is seen to be higher, three in our scanning electron micrographs and four in the transmission electron micrographs. Lindholm et al. (1988) described a bifurcation in their legend to Fig. 15, but this figure in fact shows three extrusomes emerging from the tip of a tentacle.

The "heterotrophic" type of tentacles is characterized by 23 microtubules in the tentacles. However, this type can be subdivided into two subtypes. In *M. pupula,* the tentacle axonemes are arranged in pairs and one of each pair is joined by a ribbon of microtubules. Whether or not both axonemes of a pair extend into long, emergent tentacles is presently unknown since the tentacles of *M. pupula* were retracted in the cell in our material. In *M. pulex*, however, the evidence we have gained so far indicates that all tentacle axonemes are independent of each other and extend into tentacles. Extrusomes are found in association with the basal parts of the tentacles in *M. pupula*, while in *M. pulex* the extrusomes have never been observed to be associated with tentacles. In *M. pulex* the tips of the tentacles are conical or funnel shaped (Tamar 1992). It seems probable that the tip structure of *M. pupula* is identical based on the suction cup-like appearance of the tentacle tips versus the forked end of *M. rubrum*, *M. chamaeleon*, and *M. major*.

A possible implication of these two tentacle types would be to divide the genus into two, one genus containing the heterotrophic species and the second the mixotrophic species. Yet, LM micrographs of the freshwater type species *M. acarus* show tentacles ending in a fork (Foissner et al. 1999). The structure of the tentacle tips therefore does not support the notion that the heterotrophic and mixotrophic species belong to different genera.

Cirri. The detailed construction of the cirral bases shows interesting variation among the species presently examined by TEM. A numbering system of individual ciliary bases and individual rows of ciliary bases was provided by Moestrup et al. (2012) based on observations of *M. chamaeleon* (Fig. 43). Compared to *M. chamaeleon*, *M. pulex* and the two red species lack a basal body in row III, position 1 while all other 16 positions are identical. This results in a 16-basal body cirral base in *M. pulex* and the red species, rather than the 17-basal body in *M. chamaeleon*. *M. pupula* is more aberrant. The cirral base is formed by 18 basal bodies, but not as a simple addition of an extra basal body to the 17-basal body of *M. chamaeleon*. The cirral base differs in three positions from *M. chamaeleon* and in two positions from *M. rubrum*. *M. pupula* is unique in having an extra basal body in row I, position 6 and row IV, position 4. Moreover, *M. chamaeleon* differs from the other species in having seven rather than eight cilia in the emergent part of the cirrus. The basal body in row I, position 3 grows into a short cilium only, which does not participate in the formation of the cirrus.

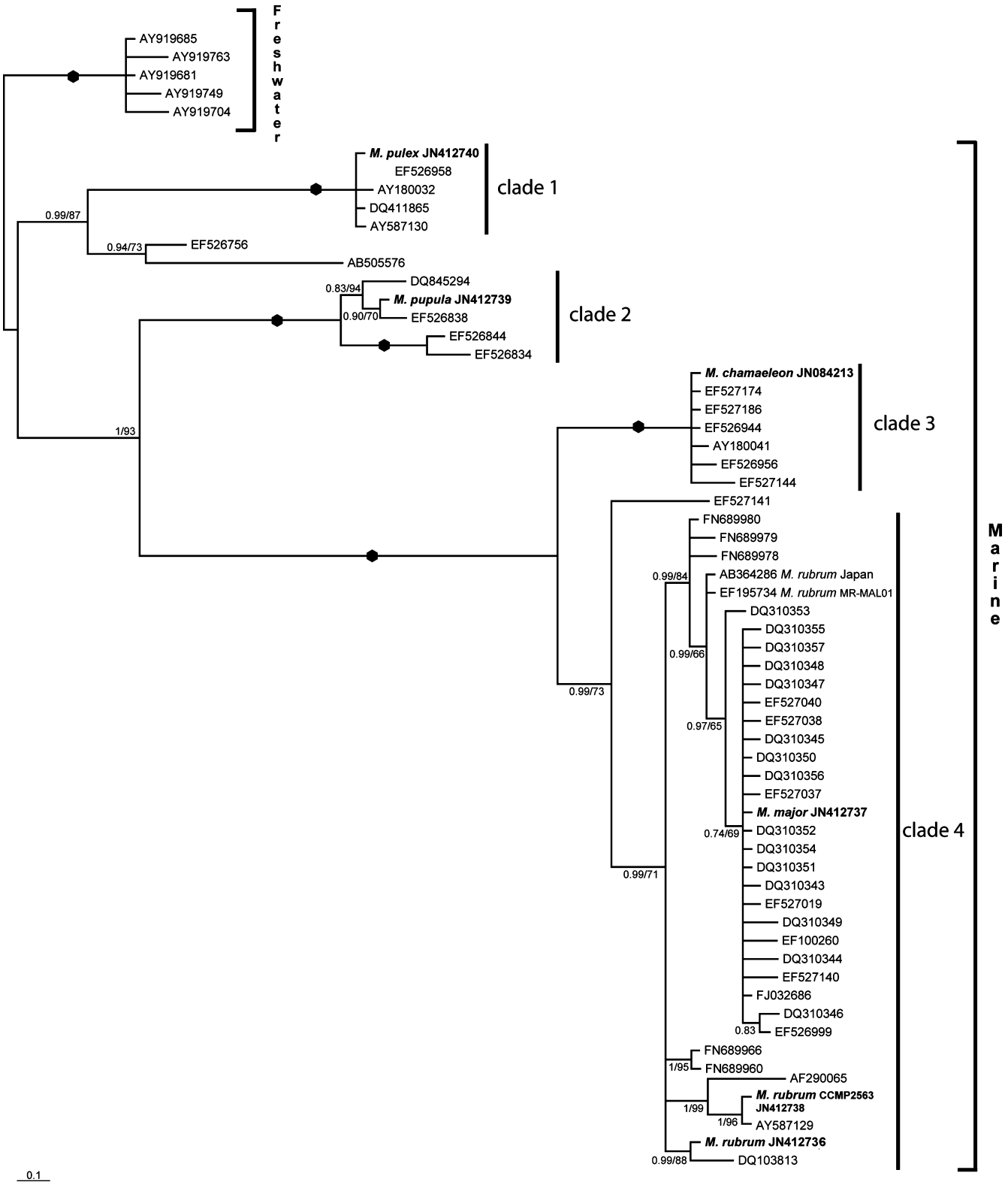

Fig. **85.** Phylogeny based on nuclear small subunit (SSU) rDNA sequences inferred from Bayesian analysis. Five freshwater *Mesodinium* environmental sequences constituted the outgroup. Branch support was obtained from Bayesian posterior probabilities and bootstrap (100 replicates) in maximum likelihood analyses. At internodes, posterior probabilities (< 1) are written first followed by bootstrap values (in percentage) from ML. The black dots represent the highest possible posterior probability (1.0) and bootstrap value (100%). Species in bold face were sequenced in this study. [Correction added after online publication July 3, 2012: The GenBank accession number of M. rubrum 41273 was changed to 412736.]

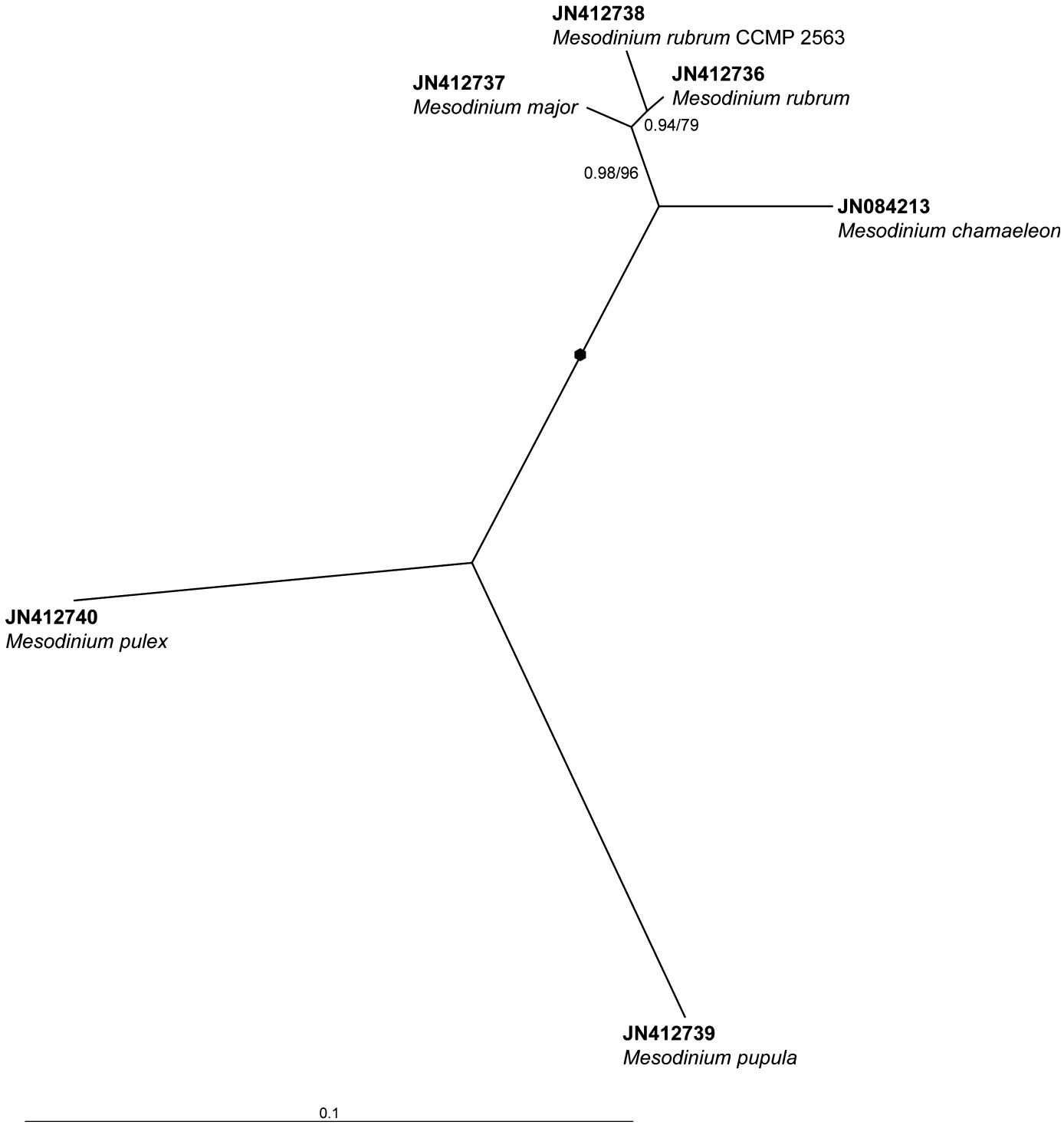

Fig. **86.** Phylogeny based on nuclear partial small subunit (SSU) rDNA, ITS region, and partial large subunit (LSU) rDNA sequences of five *Mesodinium* species inferred from Bayesian analysis. Branch support was obtained from Bayesian posterior probabilities and bootstrap (100 replicates) in maximum likelihood (ML) analyses. At internodes, posterior probabilities (< 1) are written first followed by bootstrap values (in percentage) from ML. The black dot represents the highest possible posterior probability (1.0) and bootstrap value (100%). All sequences were obtained in this study.

Fig. **87.** Phylogeny based on nuclear ITS region and partial large subunit (LSU) rDNA sequences inferred from Bayesian analysis. Branch support was obtained from Bayesian posterior probabilities and bootstrap (100 replicates) in maximum likelihood analyses. At internodes, posterior probabilities (< 1) are written first followed by bootstrap values (in percentage) from ML. The black dots represent the highest possible posterior probability (1.0) and bootstrap value (100%). All sequences obtained in this study are in bold.

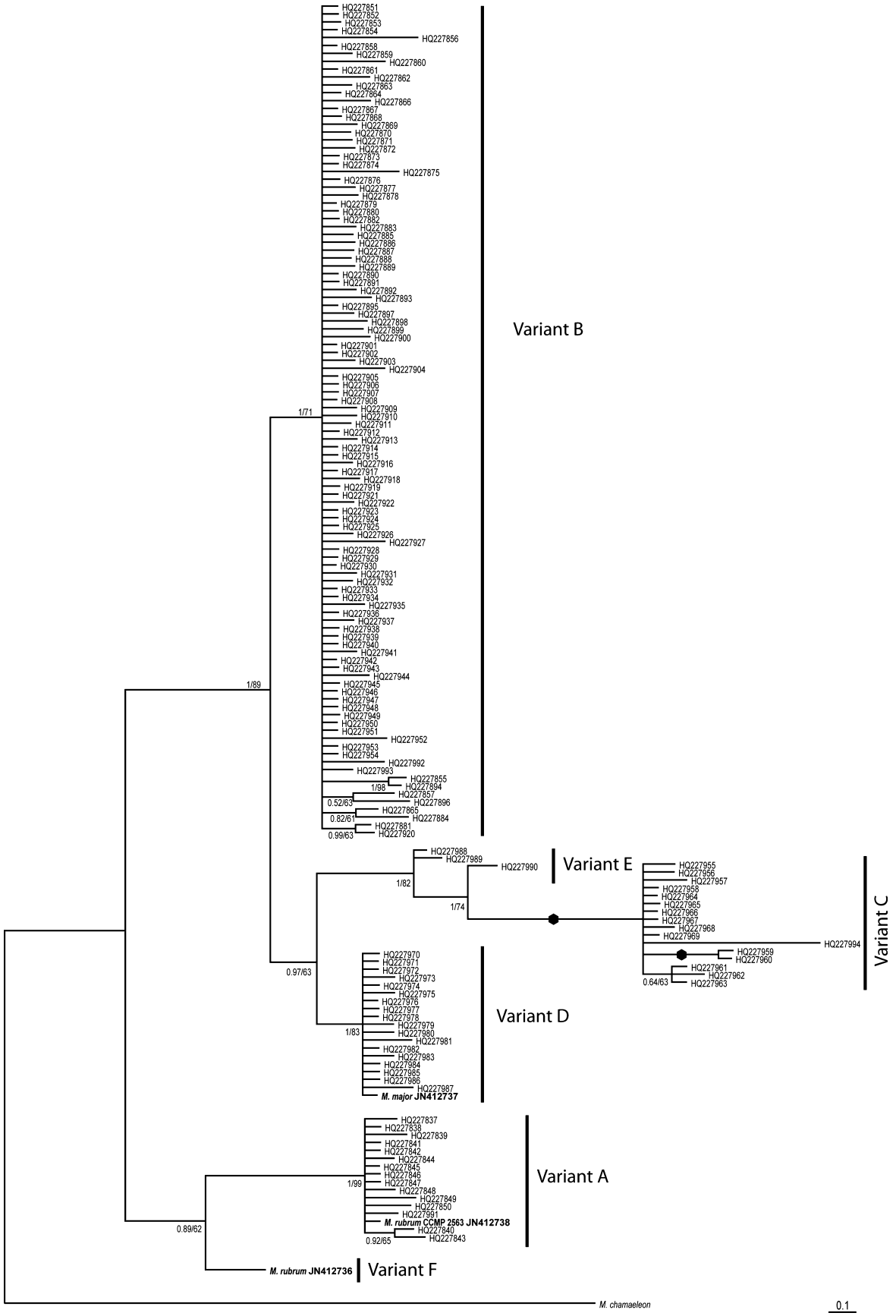
HQ227851
HQ227852
HQ227853
HQ227854
HQ227856
HQ227858
HQ227859
HQ227860
HQ227861
HQ227862
HQ227863
HQ227864
HQ227866
HQ227867
HQ227868
HQ227869
HQ227870
HQ227871
HQ227872
HQ227873
HQ227874
HQ227875
HQ227876
HQ227877
HQ227878
HQ227879
HQ227880
HQ227882
HQ227883
HQ227885
HQ227886
HQ227887
HQ227888
HQ227889
HQ227890
HQ227891
HQ227892
HQ227893
HQ227895
HQ227897
HQ227898
HQ227899
HQ227900
HQ227901
HQ227902
HQ227903
HQ227904
HQ227905
HQ227906
HQ227907
HQ227908
HQ227909
HQ227910
HQ227911
HQ227912
HQ227913
HQ227914
HQ227915
HQ227916
HQ227917
HQ227918
HQ227919
HQ227921
HQ227922
HQ227923
HQ227924
HQ227925
HQ227926
HQ227927
HQ227928
HQ227929
HQ227930
HQ227931
HQ227932
HQ227933
HQ227934
HQ227935
HQ227936
HQ227937
HQ227938
HQ227939
HQ227940
HQ227941
HQ227942
HQ227943
HQ227944
HQ227945
HQ227946
HQ227947
HQ227948
HQ227949
HQ227950
HQ227951
HQ227952
HQ227953
HQ227954
HQ227992
HQ227993
HQ227855
HQ227894
HQ227857
HQ227896
HQ227865
HQ227884
HQ227881
HQ227920
1/71
1/89
1/98
0.52/63
0.82/61
0.99/63
Variant B
HQ227988
HQ227989
HQ227990
1/82
1/74
Variant E
HQ227955
HQ227956
HQ227957
HQ227958
HQ227964
HQ227965
HQ227966
HQ227967
HQ227968
HQ227969
HQ227994
HQ227959
HQ227960
HQ227961
HQ227962
HQ227963
0.64/63
Variant C
0.97/63
HQ227970
HQ227971
HQ227972
HQ227973
HQ227974
HQ227975
HQ227976
HQ227977
HQ227978
HQ227979
HQ227980
HQ227981
HQ227982
HQ227983
HQ227984
HQ227985
HQ227986
HQ227987
M. major JN412737
1/83
Variant D
HQ227837
HQ227838
HQ227839
HQ227841
HQ227842
HQ227844
HQ227845
HQ227846
HQ227847
HQ227848
HQ227849
HQ227850
HQ227991
M. rubrum CCMP 2563 JN412738
HQ227840
HQ227843
1/99
0.92/65
Variant A
0.89/62
M. rubrum JN412736
Variant F
M. chamaeleon
0.1

Roots. In one of the red species, probably *M. rubrum* judging from the shape and the cell size provided, Grain et al. (1982) illustrated three-stranded microtubular ciliary roots associated with one of the basal bodies in each dikinetid pair. In *M. chamaeleon* we interpreted roots in a similar position to form the postciliary ribbon. We have not examined the ciliary roots in the other species but we assume that the three-stranded microtubular roots are homologous with the three-stranded microtubular root templates we observed in each of the two pairs of centrioles in *M. pupula*. The one-stranded root template associated with the other basal body in each dikinetid pair in *M. pupula* is, however, presently without any known homologue in the other species. Additional work is needed to clarify the structure and paths of the microtubular roots in *Mesodinium*. This also applies to the structure of the cirral base, in which a very complex system of cross-banded fibers connects the basal bodies with each other and with other parts of the cell.

Phylogeny. The phylogenetic relationships among *Mesodinium* species placed our five marine species into four different clades. These clades, well supported in both phylogenies, mirror the different life strategies adopted by each species. The primary force in the evolution within this genus seems to be the feeding strategy. There is a shift between the heterotrophic *M. pulex* and *M. pupula* and the plastid-bearing *M. chamaeleon*, *M. rubrum*, and *M. major*. In the SSU rDNA phylogeny, certain environmental sequences did not group within those species-defined clades and indicate the existence of other *Mesodinium* species, perhaps with different feeding strategies. For example, sequence AB505576 and sequence EF526756, grouping as a sister group to *M. pulex*, originate from microbial mats of deep-sea cold-seep sediment from Japan and from an anoxic fjord in Norway, respectively. It is possible that *Mesodinium* species living in anoxic environments may display strategies, which are different from the benthic or planktonic species studied herein. *Mesodinium pulex* and *M. pupula* never formed a clade in the various tests carried out or even when removing two sequences mentioned above (data not shown) despite their common feeding strategies. Since *M. pulex* and *M. pupula* belong to two different clades it seems reasonable to conclude that the sequence DQ845294, previously identified as *M. pulex*, represents *M. pupula*.

Mesodinium was included in the order Cyclotrichiida Jankowski, 1980 of the ciliate class Litostomatea Small & Lynn, 1981. As the class name implies, members of this class have only a simple ciliature surrounding the cytostome. However, the family Mesodiniidae Jankowski, 1980 appears to be unique in lacking kinetids associated with the cytostome. The oral opening is lined by microtubules that may serve as a cytoskeleton for this part of the cell and, as shown by Allen (1974) and Allen and Wolf (1974, 1979) for *Paramecium*, functions in the recycling of membrane material used in food uptake The only positive evidence for phylogenetic relationship between *Mesodinium* and other groups of ciliates is the structure of the ciliary transition region, which agrees with the idea that *Mesodinium* is related to or may be classified in the Litostomatea (e.g. Lynn 2010).

Class Litostomatea Small and Lynn, 1981.
Subclass Haptoria.
Order Cyclotrichiida Jankowski, 1980.
Family Mesodiniidae Jankowski, 1980.

Mesodinium major n. sp. Diagnosis. Cells 40–55 μm long and 35–50 μm wide (n = 10), divided into two unequal parts by a constriction (girdle). The oral hemisphere flattened and slightly wider than the aboral hemisphere. Chloroplasts of cryptophyte origin present in high numbers, giving the cells a reddish-brown color. The cytostome large and surrounded by tentacles supported internally by 14 microtubules. The oral end plastic, sometimes producing around the edge of the cell flaps containing chloroplasts, the so-called Medusa-form. Each cell with ~ 74 rows of polykinetid cirri. The aboral ciliary dikinetids arranged in longitudinal rows in the same number as the cirri. Each longitudinal row formed by ~ 25 pairs of cilia, terminating orally into two pairs of naked centrioles. Cells planktonic, marine.

Basionym. *Mesodinium rubrum* var. *major* p. 27 in Leegaard 1920

Etymology. Major: large, the most conspicuous feature of this species being its large size.

Type locality. Tuborg Havn, Denmark (latitude: 55°43′60.00″N; longitude: 12°34′60.00″E).

Type material. Stub for SEM deposited at the Botanical Museum, University of Copenhagen and numbered CAT 2474; GenBank accession number (JN412737); Fig. 4–7, illustrating material from the field. Culturing failed and cultures therefore not available.

Emended description of Mesodinium rubrum. Diagnosis. Cells are 25–35 μm long and 16–25 μm wide (n = 20), divided into two unequal parts by a constriction (girdle). The oral hemisphere shorter and wider than the conical aboral hemisphere. A total of 8–20 chloroplasts of cryptophyte origin present, giving the cells a brown reddish color. The cytostome, although not conspicuous, surrounded by 16 tentacles. Each of the ~ 8 μm long tentacles with ca. four extrusomes at the tip. Cells possess ~ 31–36 rows of polykinetid cirri. The aboral ciliary dikinetids arranged in longitudinal rows in the same number as the cirri. Each longitudinal row formed by ~ 16 pairs of cilia, terminating orally into two pairs of centrioles. Cells are planktonic, marine, phototrophic, and feed on cryptophytes.

Type locality. Kiel Bay (latitude: 54°22′19.89″N, longitude: 10°11′5.46″E).

Neotype. Stub for SEM deposited at the Botanical Museum, University of Copenhagen and numbered CAT 2475; GenBank accession number (JN412736). Collected at Frederikssund, Denmark (latitude: 55°50′27.65″N, longitude: 12°2′51.77″ E) 17 April 2007.

ACKNOWLEDGMENTS

We thank Lis Munk Frederiksen for expert assistance with sectioning. We also thank Prof. Denis Lynn, University of British Columbia, and Professor Klaus Hausmann, Freie Universität, Berlin, for supplying literature, and Dr. Henning Knudsen, Statens Naturvidenskabelige Museum, Copenhagen, for translation of texts from the Russian. Thanks also to Prof. Wayne Coats, Smithsonian Environmental Research Center, for comments and suggestions and Prof. Niels Peder Kristensen, University of Copenhagen, for advice on nomenclature. Dr. Niels Daugbjerg, also at University of Copenhagen, kindly let us use an inverted microscope, recently funded by Villum Kann Foundation. This study was supported by grant no 272-06-0485 from the Danish Research Council to Per Juel Hansen. A Ph.D. grant from the University of Copenhagen supported Lydia Garcia-Cuetos.

LITERATURE CITED

Aescht, E. 2001. Catalogue of the generic names of ciliates (Protozoa, Ciliophora). *Denisia*, **1**:1–350.

Allen, R. D. 1974. Food vacuole membrane growth with microtubule associated membrane transport in *Paramecium*. *J. Cell Biol.*, **63**:904–922.

Allen, R. D. & Wolf, R. W. 1974. The cytoproct of *Paramecium caudatum*: structure and function, microtubules, and fate of food vacuole membranes. *J. Cell Sci.*, **14**:611–631.

Allen, R. D. & Wolf, R. W. 1979. Membrane cycling at the cytoproct of *Tetrahymena*. *J. Cell Sci.*, **35**:217–227.

Bass, D., Brown, N., Mackenzie-Dodds, J., Dyal, P., Nierzwicki-Bauer, S. A., Vepritskiy, A. A. & Richards, T. A. 2009. A molecular perspective on ecological differentiation and biogeography of cyclotrichiid ciliates. *J.Eukaryot. Microbiol.*, **56**:559–567.

Borror, A. C. 1972. Tidal marsh ciliates (Protozoa): morphology, ecology, systematics. *Acta Protozool.*, **10**:29–71.

Bowers, H. A., Tomas, C., Tengs, T., Kempton, J. W., Lewitus, A. J. & Oldach, D. W. 2006. Raphidophyceae [Chadefaud ex Silva] systematics and rapid identification: sequence analyses and real-time PCR assays. *J. Phycol.*, **42**:1333–1348.

Crawford, D. W. 1993. Some observations on morphological variation in the red-water ciliate *Mesodinium rubrum*. *J. Mar. Biol. Assoc. U.K.*, **73**:975–978.

Dragesco, J. 1963. Compléments à la connaissance des ciliés mésopsammiques de Roscoff. I.- Holotriches. *Cah. Biol. Mar.*, **4**:91–119.

Fauré-Fremiet, E. 1924. Contribution à la connaissance des infusoires planctoniques. *Bull. Biol. Fr. Belg., Suppl.*, **6**:I–171.

Felsenstein, J. 1981. Evolutionary trees from DNA sequences: a maximum likelihood approach. *J. Mol. Evol.*, **17**:368–376.

Felsenstein, J. 1985. Confidence limits on phylogenies: an approach using the bootstrap. *Evolution*, **39**:783–791.

Foissner, W., Berger, H. & Schaumburg, J. 1999. Identification and ecology of limnetic plankton ciliates. *Informationsberichte des Bayerischen Landesamtes für Wasserwirtschaft*, Heft **3/99**:793 pp.

Garcia-Cuetos, L., Moestrup, Ø., Hansen, P. J. & Daugbjerg, N. 2010. The toxic dinoflagellate *Dinophysis acuminata* harbors permanent chloroplasts of cryptomonad origin, not kleptochloroplasts. *Harmful Algae*, **9**:25–38.

Grain, J., de Puytorac, P. & Grolière, C. A. 1982. Quelques précisions sur l'ultrastructure et la position systématique de Cilié *Mesodinium rubrum*, et sur la constitution de ses symbiontes chloroplastiques. *Protistologica*, **18**:7–21.

Guindon, S. & Gascuel, O. 2003. A simple, fast and accurate method to estimate large phylogenies by maximum-likelihood. *Syst. Biol.*, **52**:696–704.

Gustafson, D. E., Stoecker, D. K., Johnson, M. D., Van Heukelem, W. F. & Sneider, K. 2000. Cryptophyte algae are robbed of their organelles by the marine ciliate *Mesodinium rubrum*. *Nature*, **405**:1049–1052.

Hall, T. A. 1999. Bioedit: a user friendly biological sequence alignment editor and analysis program from windows 95/97/NT. *Nucleic Acids Symp. Ser.*, **41**:95–98.

Hansen, P. J. & Fenchel, T. 2006. The bloom-forming ciliate *Mesodinium rubrum* harbours a single permanent endosymbiont. *Mar. Biol. Res.*, **2**:169–177.

Hansen, G., Daugbjerg, N. & Franco, J. M. 2003. Morphology, toxin composition and LSU rDNA phylogeny of Alexandrium minutum (Dinophyceae) from Denmark, with some morphological observations on other European strains. *Harmful Algae*, **2**:317–335.

Herfort, L., Peterson, T. D., McCue, L. A., Crump, B. C., Prahl, F. G., Baptista, A. M., Campbell, V., Warnick, R., Selby, M., Roegner, G. C. & Zuber, P. 2011. *Myrionecta rubra* population genetic diversity and its cryptophyte chloroplast specificity in recurrent red tides in the Columbia River estuary. *Aquat. Microb. Ecol.*, **62**:85–97.

Huelsenbeck, J. P. & Ronquist, F. 2001. MRBAYES: Bayesian inference of phylogenetic trees. *Bioinformatics*, **17**:754–755.

Jakobsen, H. H., Everett, L. M. & Strom, S. L. 2006. Hydromechanical signaling between the ciliate *Mesodinium pulex* and motile protist prey. *Aquat. Microb. Ecol.*, **44**:197–206.

Jankowski, A. W. 1976. Revision of the systematics of cyrtophorids. *In*: Markevich, A. P. & Yu, I. (ed.), Materials II. All-Union Conference on Protozoology. Part 1, General Protozoology. Naukova Dumka, Kiev. p. 167–168.

Jankowski, A. W. 2007. Phylum Ciliophora Doflein (1901). *In*: Alimov, A. F. (ed.), Protista. Part 2, Handbook on Zoology. Russian Academy of Science, Zoological Institute, St. Petersburg. p. 415–993.

Johnson, M. D. & Stoecker, D. K. 2005. Role of feeding in growth and photophysiology of *Myrionecta rubra*. *Aquat. Microb. Ecol.*, **39**:303–312.

Johnson, M. D., Oldach, D., Delwiche, C. F. & Stoecker, D. K. 2007. Retention of transcriptionally active cryptophyte nuclei by the ciliate *Myrionecta rubra*. *Nature*, **445**:426–428.

Johnson, M. D., Tengs, T., Oldach, D. & Stoecker, D. K. 2006. Sequestration, performance, and functional control of cryptophyte plastids in the ciliate *Myrionecta rubra* (Ciliophora). *J. Phycol.*, **42**:1235–1246.

Johnson, M. D., Tengs, T., Oldach, D. W., Delwiche, C. F. & Stoecker, D. K. 2004. Highly divergent SSU rRNA genes found in the marine ciliates *Myrionecta rubra* and *Mesodinium pulex*. *Protist*, **155**:347–359.

Kahl, A. 1935. Urtiere oder Protozoa I: Wimpertiere oder Ciliata (Infusoria). 4. Peritricha und Chonotricha. *In*: Dahl, F. (ed.), Die Tierwelt Deutschlands und der angrenzenden Meeresteile, Gustav Fischer, Jena. p. 651–886.

Katoh, K. & Toh, H. 2008. Recent developments in the MAFFT multiple sequence alignment program. *Brief. Bioinform.*, **9**:286–298.

Krainer, K. H. & Foissner, W. 1990. Revision of the genus *Askenasia* Blochmann, 1895, with proposal of two new species, and description of *Rhabdoaskenasia minima* n.g., n. sp. (Ciliophora, Cyclotrichida). *J. Protozool.*, **37**:414–427.

Leegaard, C. 1920. Mikroplankton from the Finnish waters during the month of May 1912. *Acta Soc. Fauna Flora Fenn.*, **48**:1–41.

Lindholm, T. 1985. *Mesodinium rubrum*—a unique photosynthetic ciliate. *Adv. Aquat. Microbiol.*, **3**:1–48.

Lindholm, T., Lindroos, P. & Mörk, A.-C. 1988. Ultrastructure of the photosynthetic ciliate *Mesodinium rubrum*. *Biosystems*, **21**:141–149.

Lohmann, H. 1908. Untersuchungen zur Feststellung des vollständigen Gehaltes des Meeres an Plankton. Wissensch. Meeresunters. *Biol. Anstalt Helgoland*, **10**:130–370.

Lynn, D. H. 2010. Ciliated Protozoa: Characterization, Classification, and Guide to the Literature. Springer, Dordrecht. 605 p.

Moestrup, Ø., Garcia-Cuetos, L., Hansen, P. J. & Fenchel, T. 2012. Studies on the genus *Mesodinium*. I. Ultrastructure and description of M. chamaeleon sp. nov., a benthic marine species with green or red chloroplasts. *J. Eukaryot. Microbiol.*, **59**:20–39.

Nunn, G. B., Theisen, B. F., Christensen, B. & Arctander, P. 1996. Simplicity-correlated size growth of the nuclear 28S ribosomal RNA D3 expansion segment in the crustacean order Isopoda. *J. Mol. Evol.*, **42**:211–223.

Park, J. S., Myung, G., Kim, H. S., Cho, B. C. & Yih, W. 2007. Growth responses of the marine photosynthetic ciliate *Myrionecta rubra* to different cryptomonad strains. *Aquat. Microb. Ecol.*, **48**:83–90.

Posada, D. 2008. jModelTest: phylogenetic model averaging. *Mol. Biol. Evol.*, **25**:1253–1256.

Scholin, C. A., Herzog, M., Sogin, M. & Anderson, D. M. 1994. Identification of group-specific and strain-specific genetic markers for globally distributed *Alexandrium* (Dinophyceae).II. Sequence analysis of a fragement of the LSU ribosomal RNA gene. *J. Phycol.*, **30**:999–1011.

Strüder-Kypke, M. C., Wright, A.-D. G., Foissner, W., Chatzinotas, A. & Lynn, D. H. 2006. Molecular phylogeny of litostome ciliates (Ciliophora, Litostomatea) with emphasis on free-living haptorian genera. *Protist*, **157**:261–278.

Swofford, D. L. 2002. PAUP* 4.0: Phylogenetic Analysis Using Parsimony (*And Other Methods). Sinauer Associates, Sunderland, Massachusetts.

Tamar, H. 1987. On division in a fresh-water *Mesodinium acarus*. *Acta Protozool.*, **26**:213–218.

Tamar, H. 1992. Four marine species of *Mesodinium* (Ciliophora: Mesodiniidae). II. Mesodinium pulex Clap. & Lachm., 1858. *Arch. Protistenk.*, **141**:284–303.

Taylor, F. J. R., Blackbourn, D. J. & Blackbourn, J. 1971. The red water ciliate *Mesodinium rubrum* and its incomplete symbionts: a

review including new ultrastructural observations. *J. Fish. Res. Board Canada*, **28**:391–407.
Wilgenbusch, J. C., Warren, D. L. & Swofford, D. L. 2004. AWTY: a system for graphical exploration of MCMC convergence in Bayesian phylogenetic inference. Available at http://ceb.csit.fsu.edu/awty.
Yang, Z. & Rannala, B. 1997. Bayesian phylogenetic inference using DNA sequences: a Markov Chain Monte Carlo method. *Mol. Biol. Evol.*, **14**:717–724.

Received: 01/10/12, 03/02/12; accepted: 03/02/12